SAR TESTING OF AMBIT MICROSYSTEMS MODEL T60H677 802.11 a/b MINI PCI WITH THREE HOST COMPUTERS

AMBIT MODEL: T60H677
FCC ID: MCLT60H677

Host Computers:

1. Quantatw Model ZG1S with Ambit Model ZG1S 802.11a antenna (PC Serial #QCHCP025000023)
2. Quantatw Model ZI1S with Ambit Model ZI1S 802.11a antenna (PC Serial #QCHCOU24800018)
3. Compal Model L1S with Ambit Model BY27 802.11a antenna (PC Serial #BBY27001004)

February 25, 2003

Prepared for: Ambit Microsystems Corporation
4-1, Ming-Sheng Street
Tu-Cheng Industrial Area
Tu-Cheng City, Taiwan, R.O. C.

Prepared by: Om P. Gandhi
Professor of Electrical and Computer Engineering
University of Utah
50 S Central Campus Dr., Rm. 3280
Salt Lake City, UT 84112-9206

TABLE OF CONTENTS

SAR TESTING OF AMBIT MICROSYSTEMS MODEL T60H677 802.11 a/b MINI PCI WITH THREE HOST COMPUTERS

AMBIT MODEL: T60H677
FCC ID: MCLT60H677

Host Computers:

1. Quantatw Model ZG1S with Ambit Model ZG1S 802.11a antenna (PC Serial #QCHCP025000023)
2. Quantatw Model ZI1S with Ambit Model ZI1S 802.11a antenna (PC Serial #QCHCOU24800018)
3. Compal Model L1S with Ambit Model BY27 802.11a antenna (PC Serial #BBY27001004)

I. Introduction

The U.S. Federal Communications Commission (FCC) has adopted limits of human exposure to RF emissions from mobile and portable devices that are regulated by the FCC [1]. The FCC has also issued Supplement C (Edition 97-01) to OET Bulletin 65 [2] and a more recent version of the same [3] defining both the measurement and the computational procedures that should be followed for evaluating compliance of mobile and portable devices with FCC limits for human exposure to radiofrequency emissions.

We have used the measurement procedure for SAR compliance testing of the Ambit Microsystems Model T60H677 802.11 a/b Mini PCI built into three host computers. These host computers shown in Figs. 1-3, respectively, are:

1. Quantatw Model ZG1S.
2. Quantatw Model ZI1S.
3. Compal Model L1S.

For each of the host computers, the approximate locations of the corresponding 802.11a wireless antennas built into the keyboard are indicated by a sticker in parts c of each of the Figs. 1-3, respectively. The Ambit Model T60H677 PCI with slightly different 802.11a antennas for each of the three host computers operates over the frequency band 5.17-5.81 GHz in the normal mode with conducted powers given for the individual host computers in Tables 1-3, respectively.

For SAR measurements, three configurations of each of the wireless PCs relative to the experimental phantom have been used. These are as follows:

a. **Configuration 1** is for the wireless PC placed on a user's lap. For this configuration, a planar phantom model with inside dimensions 12" x 16.5" (30.5 x 41.9 cm) and a base thickness of 2.0 ± 0.2 mm (recommended in [3]) was used for SAR measurements and the bottom side of each of the laptop computers shown in parts b of Figs. 1, 2, and 3 was pressed against it. See, for example, Fig. 4 where the bottom of Quantatw Model ZG1S PC is pressed against the base of the planar phantom. Due to the possible shielding effect of the keyboard, the measured SARs were fairly low and were, in fact, close to the noise level of the measuring system (estimated to be on the order of 0.02 W/kg) for Quantatw Model ZI1S and Compal Model L1S host computers.

b. For a bystander, the SAR values were determined for Configurations 2 and 3 of the PCs relative to the flat phantom. These configurations are:

   Configuration 2: Edge-on placement of the PC with the antenna edge (right edge) at 90° pressed against the bottom of the planar phantom with separation of 0 cm for Quantatw Models ZG1S and ZI1S (see Figs. 7 and 8), and at a distance of 1.5 cm for Compal Model L1SPC (see Fig. 9). Because of a larger SAR for the Compal Model L1S PC for this configuration, a spacing of 1.5 cm rather than 0 cm was used for this PC. This configuration 2 for SAR testing represents the case of a bystander standing to the right of the PC with a separation of 0 cm from the antenna edge for Quantatw Models ZG1S and ZI1S PCs and 1.5 cm for Compal Model L1S PC. It should be noted that a spacing of 1.5-2.5 cm is suggested in [3] for end-on testing of SARs.

   Configuration 3: End-on placement of the PC with the broader back edges of three host computers at 90° pressed against the bottom of the planar phantom with separation of 0 cm (see Figs. 10-12). This represents the case of a bystander behind the PC screen with separation of 0 cm from the PC edge.

II. The SAR Measurement System

The University of Utah SAR Measurement System has been described in peer-reviewed literature [Ref. 8 -- attached here as Appendix A]. A photograph of the SAR Measurement System is given in Fig. 5. This SAR Measurement System uses a computer-controlled 3-D stepper motor system (Arrick Robotics MD-2A). A triaxial Narda Model 8021 E-field probe is used to determine the internal electric fields. The positioning repeatability of the stepper motor system moving the E-field probe is within ±0.1 mm. Outputs from the three channels of the E-field probe are dc voltages, the sum of which is proportional to the square of the internal electric fields $\left(|E_i|^2\right)$ from which the SAR can be obtained from the equation SAR = $\sigma\left(|E_i|^2\right)\Big/\rho$, where σ and ρ are the conductivity and mass density of the tissue-simulant materials, respectively [5]. The dc voltages for the three channels of the E-field probe are read by three HP 34401A multimeters and sent to the computer via an HPIB interface. The setup is carefully grounded and shielded to reduce the noise due to the electromagnetic interference (EMI). A cutout in a wooden table of dimensions 38.1 × 21.6 cm allows placement of a plastic holder (shown in Fig. 6) on which the host computers with the Ambit 802.11 a/b Wireless Antennas (see Figs. 1, 2, and 3) are supported. A plastic holder (see Fig. 6) can be moved up or down so that the base of the PC (for Configuration 1) is pressed against the base of the flat phantom for determination of SAR for above-lap position. Similarly, for "end-on" SAR determination, Configuration 2, the laptop computer screen is mounted sideways (at 90°) on the plastic holder and moved up so that the edge of the PC with the 802.11 a/b Wireless Antennas was pressed against the bottom of the flat phantom with a spacing of 0 or 1.5 cm (see Figs. 7, 8, and 9). A second bystander, Configuration 3, where an individual may be behind the PC screen at a distance of 0 cm from the broader edge of the PC (see Figs. 10, 11, and 12) was also used for SAR measurements.

The Flat Phantom

As recommended in Supplement C Edition 01-01 to OET Bulletin 65 [3], a planar phantom model with inside dimensions 12" × 16.5" (30.5 × 41.9 cm) and base thickness 2.0 ± 0.2 mm was used for SAR measurements (see Figs. 4 and 7-12).

III. Calibration of the E-Field Probe

The IEEE Draft Standard P1528 [4] suggests a recommended procedure for probe calibration (see Section 4.4.1 of [4]) for frequencies above 800 MHz where waveguide size is manageable. Calibration using a rectangular waveguide is recommended. As in some previously reported SAR measurements at 6 GHz [5], we have calibrated the Narda Model 8021 Miniature Broadband Electric Field Probe of tip diameter 4 mm (internal dipole dimensions on the order of 2.5 mm) using a rectangular waveguide WR 159 (of internal dimensions 1.59 x 0.795 inches) that was filled with the tissue-simulant fluid of composition given in Section V (see Figs. 13a,b). The triaxial (3 dipole) E-field probe shown in Fig. 14 was originally developed by Howard Bassen and colleagues of FDA and has been manufactured under license by Narda Microwave Corporation, Hauppage, New York. The probe is described in detail in references 6 and 7. It uses three orthogonal pick up dipoles each of length about 2.5 mm offset from the tip by 3 mm, each with its own leadless zero voltage Schottky barrier diode operating in the square law region. The sum of the three diode outputs read by three microvoltmeters [8] gives an output proportional to E^2. By rotating the probe around its axis, the isotropy of the probe was measured to be less than ± 0.23 dB and the deviation of the probe from the square law behavior was less than ± 3%.

As suggested in the Draft Standard P1528, the waveguide (WR 159) filled with the tissue-simulant fluid was maintained vertically. From microwave field theory [see e.g. ref. 9], the transverse field distribution in the liquid corresponds to the fundamental mode (TE_{10}) with an exponential decay in the vertical direction (z-axis). The liquid level was 15 cm deep which is deep enough to guarantee that reflections from the top liquid surface do not affect the calibration. By comparing the square of the decaying electric fields expected in the tissue from the analytical expressions for the TE_{10} mode of the rectangular waveguide, we obtained a calibration factor of

2.98 (mW/kg)/μV with a variability of less than ±2% for measurement frequencies of 5.2, 5.3, 5.7 and 5.8 GHz, respectively. This is no doubt due to a fairly limited frequency band of only 0.6 GHz out of a recommended bandwidth of 2.2 GHz for the TE_{10} mode for the WR159 waveguide (recommended band of 4.9-7.1 GHz -- see e.g. ref. 9) and the fact that the bandwidth of 600 MHz for the entire set of measurements is on the order of ± 5.5% of the midband frequencies..

The date for the calibration of the E-field probe closest to the SAR tests given here was February 21, 2003.

IV. SAR System Verification

Since we do not have a dipole for the 5 GHz band, a half wave dipole at 1900 MHz was used instead for SAR system verification. This dipole of length 76.0 mm and diameter 1.5 mm and h = 39.5 mm is shown in Fig. 15. As recommended in OET65 Supplement C [3], we used a spacing of 10 mm from the dipole to the tissue-simulant fluid composed of 40.4% water, 58.0% sugar, 0.5% salt (NaCl), 1% HEC, and 0.1% bactericide. The microwave circuit arrangement used for system verification is sketched in Fig. 16. The dielectric properties for this body-simulant fluid were measured using the Hewlett Packard (HP) Model 85070 B Dielectric Probe (rated frequency band 200 MHz to 20 GHz in conjunction with HP Model 8720C Network Analyzer (50 MHz-20 GHz) using a procedure detailed in Section V. The measured dielectric parameters of the body-simulant fluid at 1900 MHz are $\varepsilon_r = 53.1 \pm 1.3$ and $\sigma = 1.44 \pm 0.09$ S/m. The measured properties are close to the values of $\varepsilon_r = 54.0$ and $\sigma = 1.45$ S/m given in OET Supplement C [3].

The measured SAR distribution for the peak 1-g SAR region using this system verification dipole for the day of SAR measurements February 21, 2003 is given in Appendix B. Also given in Appendix B is the dipole SAR plot for this date of device testing. The peak 1-g SAR is 35.979. The measured 1-g SAR is in excellent agreement with the FDTD-calculated 1-g SAR of 35.8 W/kg for this dipole. Also as expected, the measured SAR plot is quite symmetric.

V. Tissue Simulant Fluid for the Frequency Band 5.2 to 5.8 GHz

In OET 65 Supplement C [3], the dielectric parameters suggested for body phantom are given only for 3000 and 5800 MHz. These are listed in Table 4 here. Using linear interpolation, we can obtain the dielectric parameters to use for the frequency band between 5.2 to 5.8 GHz. The desired dielectric properties thus obtained are also given in Table 4. From Table 4, it can be noticed that the desired dielectric constant ε_r varies from 48.2 to 49.0 which is a variation of less than ± 1% from the average value of 48.6 for this band. Also the conductivity σ varies linearly with frequency from 5.3 to 6.00 S/m. For the SAR measurements given in this report, we have used a tissue-simulant fluid developed at the University of Utah which consists of 68.0% water, 31.0% sugar and 1% HEC. For this composition, we have measured the dielectric properties using a Hewlett Packard (HP) Model 85070B Dielectric Probe in conjunction with HP Model 8720C Network Analyzer (50 MHz-20 GHz). The measured dielectric properties at a mid band frequency of 5.30 GHz are as follows: $\varepsilon_r = 48.5 \pm 1.7$ and $\sigma = 5.40 \pm 0.08$ S/m. From Table 4, we obtain the desired dielectric properties to simulate the body tissue at the midband frequency of 5.30 GHz to be $\varepsilon_r = 48.9$ and $\sigma = 5.42$ S/m. Thus, the measured properties for the body-simulant fluid are close to the desired values. Also as expected, the conductivity of this fluid varies linearly with frequency rising to 6.03 ± 0.09 S/m at 5.8 GHz, while the dielectric constant ε_r is nearly the same as the measured value at 5.3 GHz.

The procedure is as follows: The HP Model 95070B Dielectric Probe (see Fig. 17) is an open-circuited transmission-line (coaxial line) probe similar to that described in Section B.1.2 of the Draft IEEE Standard 1528 [4]. The theory of the open-circuited coaxial line method has been described in scientific literature [10-12]. We have previously used this method in determining the dielectric properties of tissue-simulant materials at 6 GHz [5]. In this method, the complex reflection coefficient Γ^* measured for the open end of the coaxial line can be used to calculate the complex permittivity ε^* from the following equation [5]

$$\varepsilon^* = \frac{1-\Gamma^*}{j\omega Z_o C_o\left(1+\Gamma^*\right)} - \frac{C_f}{C_o} \tag{1}$$

where Z_o is the characteristic impedance (50 Ω) for the coaxial line, C_o is the capacitance when the line is in air and C_f is the capacitance that accounts for the fringing fields in the dielectric of the coaxial line.

For the HP85070B Dielectric Probe with diameters of the outer and inner conductors 2b = 3.00 mm and 2a = 0.912 mm, respectively, the following capacitances were obtained using deionized water and methanol as the calibration fluids. The following capacitances were obtained:

$$C_o = 0.022 \text{ pF}$$

$$C_f = 0.005 \text{ pF}$$

Using the network analyzer HP8720C, we measured the reflection coefficient Γ^* for the open end of the coaxial line that was submerged in the tissue-simulant fluid. Using Eq. 1, the complex permittivity of the fluid was measured at various frequencies 5.2-5.8 GHz. From the imaginary part of the complex permittivity $\text{Im}(\varepsilon^*)$, we can obtain the conductivity σ from the relationship

$$\sigma = \frac{\text{Im}(\varepsilon^*)}{\omega\varepsilon_o} \tag{2}$$

VI. The Measured SAR Distributions

The RF power outputs measured for the three PCs for the normal mode used with these PCs are given in Tables 1 to 3, respectively. For SAR measurements, we selected frequencies of 5.20, 5.30, and 5.745 GHz. The various frequencies were selected both for their highest power outputs as well as to cover the different frequency bands planned for these PCs. As recommended in Supplement C, Edition 01-01 [3], the stability of the conducted power was determined by repeated SAR measurements at the same location for each of the selected

channels. The variability of the SAR thus determined for three repeated measurements over a 60-minute time period was within ± 0.1 dB (± 2.5%).

The highest SAR region for each of the measurement frequencies was identified in the first instance by using a coarser sampling with a step size of 8.0 mm over three overlapping areas for a total scan area of 8.0 × 9.6 cm. The data thus obtained was resolved into a 4 x 4 times larger grid i.e. a grid involving 40 x 28 points by linear interpolation using a 2 mm step size. After thus identifying the region of the highest SAR, the SAR distribution was then measured with a resolution of 2 mm in order to obtain the peak 1 cm^3 or 1-g SAR. The SAR measurements were performed at 4, 6, 8, 10, 12 mm height from the bottom surface of the body-simulant fluid. The SARs thus measured were extrapolated using a second-order least-square fit to the measured data to obtain values at 1, 3, 5, 7 and 9 mm height and used to obtain 1-g SARs. The uncertainty analysis of the University of Utah SAR measurement system is given in Appendix C. The combined standard uncertainty is ± 8.3%.

As shown in Figs. 1, 2, and 3 parts c, the Ambit 802.11a Wireless Antennas are built into the base of the PC close to the right edges. On account of the relative shielding effects of the keyboard and other circuitry in the base of the PCs, the SARs for several exposure conditions defined as Configurations 1, 2, and 3 in Section I were fairly low. For several of these exposure configurations, the SARs were too low to measure and within the noise levels for the SAR measurement system (~ 0.02 W/kg). For the exposure configurations where the SARs were measurable, the coarse scan measurements are given in Figs. 18, 19, and 20, respectively. In these figures, the two axes are marked in units of step size of 8 mm. The highest SAR regions shown in maroon color are above the regions of the radiating 802.11a antenna for each of the PCs. Given in Tables 5-13 are the SAR distributions for the peak SAR regions of volume 10 ×10 × 10 mm for which the coarse scans are given in Figs. 18-20,a-c, respectively. The SARs are given for xy planes at heights z of 1, 3, 5, 7, and 9 mm from the bottom of the flat phantom. The individual SAR values for this grid of 5 × 5 × 5 or 125 points are averaged to obtain peak 1-g SAR values (for a volume of 1 cm^3). The temperature variation of the tissue-simulant fluid

measured with a Bailey Instruments Model BAT 8 Temperature Probe over the 80-minute period needed for measurements at the four frequencies was 23.1 ± 0.2°C. The z-axis scan plots taken at the highest SAR locations for each set of tests are given in Figs. 21-23, respectively.

The peak 1-g SARs for the various configurations of the three PCs; namely, Quantatw Models ZG1S and ZI1S and Compal Model L1S are summarized in Tables 14, 15, and 16, respectively. All of the measured 1-g SARs are less than the FCC 96-326 guideline of 1.6 W/kg.

VII. Comparison of the Data with FCC 96-326 Guidelines

According to the FCC 96-326 Guideline [1], the peak 1-g SAR for any 1-g of tissue should not exceed 1.6 W/kg. For the Ambit Microsystems Model T60H677 802.11a Mini PCI built into three host computers (Quantatw Models ZG1S and ZI1S and Compal Model L1S), the measured peak 1-g SARs are given in Tables 14, 15, and 16, respectively. The measured peak 1-g SARs vary from nearly 0 to 0.424 W/kg which are smaller than 1.6 W/kg.

REFERENCES

1. Federal Communications Commission, "Guidelines for Evaluating the Environmental Effects of Radiofrequency Radiation," FCC 96-326, August 1, 1996.

2. K. Chan, R. F. Cleveland, Jr., and D. L. Means, "Evaluating Compliance With FCC Guidelines for Human Exposure to Radiofrequency Electromagnetic Fields," Supplement C (Edition 97-01) to OET Bulletin 65, December, 1997. Available from Office of Engineering and Technology, Federal Communications Commission, Washington D.C., 20554.

3. Federal Communications Commission "Supplement C Edition 01-01 to OET Bulletin 65 Edition 97-01" June 2001.

4. IEEE Draft Standard P1528, "Recommended Practice for Determining the Peak Spatial-Average Specific Absorption Rate (SAR) in the Human Body Due to Wireless Communication Devices: Experimental Techniques," Draft CBD1.0, April 4, 2002 (IEEE Standards Coordinating Committee 34).

5. O. P. Gandhi and J-Y. Chen, "Electromagnetic Absorption in the Human Head from Experimental 6-GHz Handheld Transceivers," *IEEE Transactions on Electromagnetic Compatibility*, Vol. 39(4), pp. 547-558, 1995.

6. H. Bassen. M. Swicord, and J. Abita, "A Miniature Broadband Electric Field Probe," Ann. New York Academy of Sciences, Vol. 247, pp. 481-493, 1974.

7. H. Bassen and T. Babij, "Experimental Techniques and Instrumentation," Chapter 7 in *Biological Effects and Medical Applications of Electromagnetic Energy*, O. P. Gandhi, Editor, Prentice Hall Inc., Englewood Cliffs, NJ, 1990.

8. Q. Yu, O. P. Gandhi, M. Aronsson, and D. Wu, "An Automated SAR Measurement System for Compliance Testing of Personal Wireless Devices," *IEEE Transactions on Electromagnetic Compatibility,* Vol. 41(3), pp. 234-245, August 1999 (attached as Appendix A).

9. O. P. Gandhi, *Microwave Engineering and Applications,* Pergamon Press, New York, 1981.

10. T. W. Athey, M. A. Stuchly, and S. S. Stuchly, "Measurement of Radiofrequency Permittivity of Biological Tissues with an Open-Circuited Coaxial Line - Part I," *IEEE Transactions on Microwave Theory and Techniques*, Vol. MTT-30, pp. 82-86, 1982.

11. M. A. Stuchly, T. W. Athey, G. M. Samaras, and G. E. Taylor, "Measurement of Radiofrequency Permittivity of Biological Tissues with an Open-Circuited Coaxial Line -

Part II - Experimental Results," *IEEE Transactions on Microwave Theory and Techniques*, Vol. MTT-30, pp. 87-92, 1982.

12. C. L. Pournaropoulos and D. K. Misra, "The Coaxial Aperture Electromagnetic Sensor and Its Application for Material Characterization," *Measurement Science and Technology*, Vol. 8, pp. 1191-1202, 1997.

Table 1. Average conducted RF power outputs measured at various frequencies for the Quantatw Model ZG1S PC with Ambit Model ZG1S 802.11a Wireless Antenna for the normal mode used for this PC.

Band	Channel (MHz)	Field Strength* (dBuV)	Conducted RF Power (dBm)
Low	Low CH: 5170 Mid CH: 5200 High CH: 5250	101.4 101.3 99.8	15.33 15.67 15.5
Mid	Low CH: 5250 Mid CH: 5300 High CH: 5330	99.8 100.9 102.5	16.31 16.83 16.67
High	Low CH: 5745 Mid CH: 5775 High CH: 5810	96.6 94.7 96.8	16.89 16.5 16.67

* Field strength at 3 m.

Table 2. Average conducted RF power outputs measured at various frequencies for the Quantatw Model ZI1S PC with Ambit Model ZI1S 802.11a Wireless Antenna for the normal mode used for this PC.

Band	Channel (MHz)	Field Strength* (dBuV)	Conducted RF Power (dBm)
Low	Low CH: 5170 Mid CH: 5200 High CH: 5250	92.5 94.9 92	15.33 15.67 15.5
Mid	Low CH: 5250 Mid CH: 5300 High CH: 5330	92 94.5 94.3	16.31 16.83 16.67
High	Low CH: 5745 Mid CH: 5775 High CH: 5810	94.4 90.7 93.2	16.89 16.5 16.67

* Field strength at 3 m.

Table 3. Average conducted RF power outputs measured at various frequencies for the Compal Model L1S PC with Ambit Model BY27 802.11a Wireless Antenna for the normal mode used for this PC.

Band	Channel (MHz)	Field Strength* (dBuV)	Conducted RF Power (dBm)
Low	Low CH: 5170 Mid CH: 5200 High CH: 5250	96.3 96.2 95.5	15.33 15.67 15.5
Mid	Low CH: 5250 Mid CH: 5300 High CH: 5330	95.5 95.3 94.9	16.31 16.83 16.67
High	Low CH: 5745 Mid CH: 5775 High CH: 5810	92.6 94.7 94.4	16.89 16.5 16.67

* Field strength at 3 m.

Table 4. Dielectric parameters for body phantom for the frequency band 5.2 to 5.8 GHz [3].

Frequency GHz	ε_r	σ S/m	Reference
3.0	52.0	2.73	Ref. 3
5.8	48.2	6.00	Ref. 3
5.2	49.0	5.30	Interpolated
5.3	48.9	5.42	Interpolated
5.4	48.7	5.53	Interpolated
5.6	48.5	5.77	Interpolated
5.7	48.3	5.88	Interpolated

Table 5. **Above-lap position (Configuration 1).** The SARs measured for the Quantatw Model ZG1S PC with built-in Ambit Model ZG1S 802.11a Antenna for the normal mode at 5.20 GHz (see Fig. 4).

1-g SAR = 0.114 W/kg

a. At depth of 1 mm

0.137	0.161	0.148	0.172	0.170
0.148	0.166	0.156	0.187	0.143
0.143	0.146	0.138	0.130	0.168
0.131	0.144	0.138	0.149	0.137
0.161	0.148	0.143	0.154	0.141

b. At depth of 3 mm

0.121	0.135	0.129	0.143	0.143
0.128	0.137	0.132	0.152	0.123
0.116	0.115	0.120	0.116	0.137
0.116	0.122	0.118	0.122	0.117
0.131	0.125	0.125	0.129	0.119

c. At depth of 5 mm

0.107	0.115	0.113	0.119	0.122
0.112	0.114	0.113	0.124	0.107
0.095	0.092	0.106	0.104	0.112
0.104	0.105	0.101	0.101	0.102
0.109	0.106	0.111	0.110	0.102

d. At depth of 7 mm

0.097	0.100	0.102	0.102	0.105
0.099	0.099	0.101	0.104	0.093
0.083	0.076	0.094	0.093	0.095
0.094	0.092	0.089	0.084	0.091
0.094	0.093	0.100	0.096	0.090

e. At depth of 9 mm

0.090	0.090	0.094	0.090	0.094
0.090	0.090	0.095	0.092	0.083
0.077	0.067	0.086	0.084	0.086
0.086	0.084	0.082	0.073	0.085
0.087	0.083	0.093	0.089	0.083

Table 6. **Above-lap position (Configuration 1).** The SARs measured for the Quantatw Model ZG1S PC with built-in Ambit Model ZG1S 802.11a Antenna for the normal mode at 5.30 GHz (see Fig. 4).

1-g SAR = 0.084 W/kg

a. At depth of 1 mm

0.108	0.087	0.108	0.113	0.077
0.091	0.093	0.087	0.110	0.110
0.114	0.115	0.092	0.110	0.111
0.116	0.093	0.086	0.098	0.087
0.117	0.102	0.101	0.101	0.110

b. At depth of 3 mm

0.091	0.080	0.095	0.099	0.077
0.082	0.083	0.084	0.091	0.091
0.100	0.093	0.085	0.095	0.091
0.092	0.082	0.081	0.084	0.076
0.096	0.092	0.085	0.086	0.090

c. At depth of 5 mm

0.078	0.074	0.085	0.084	0.074
0.075	0.075	0.080	0.077	0.077
0.088	0.077	0.079	0.081	0.075
0.075	0.073	0.076	0.073	0.068
0.080	0.084	0.077	0.076	0.070

d. At depth of 7 mm

0.068	0.069	0.077	0.073	0.071
0.070	0.068	0.074	0.067	0.067
0.080	0.065	0.074	0.070	0.065
0.065	0.065	0.070	0.064	0.062
0.071	0.078	0.067	0.069	0.062

e. At depth of 9 mm

0.063	0.066	0.071	0.067	0.065
0.065	0.063	0.066	0.062	0.062
0.075	0.058	0.069	0.061	0.061
0.061	0.059	0.065	0.057	0.059
0.068	0.074	0.055	0.057	0.056

Table 7. **Above-lap position (Configuration 1).** The SARs measured for the Quantatw Model ZG1S PC with built-in Ambit Model ZG1S 802.11a Antenna for the normal mode at 5.745 GHz (see Fig. 4).

1-g SAR = 0.057 W/kg

a. At depth of 1 mm

0.085	0.095	0.082	0.071	0.086
0.096	0.091	0.089	0.069	0.094
0.079	0.066	0.103	0.085	0.101
0.075	0.094	0.067	0.086	0.072
0.088	0.103	0.114	0.080	0.100

b. At depth of 3 mm

0.070	0.069	0.059	0.054	0.062
0.076	0.071	0.072	0.052	0.063
0.063	0.053	0.074	0.072	0.075
0.061	0.066	0.052	0.058	0.058
0.067	0.074	0.088	0.078	0.070

c. At depth of 5 mm

0.056	0.049	0.042	0.041	0.043
0.059	0.054	0.056	0.039	0.040
0.050	0.043	0.051	0.061	0.055
0.050	0.045	0.040	0.038	0.047
0.051	0.051	0.067	0.066	0.053

d. At depth of 7 mm

0.045	0.033	0.030	0.032	0.031
0.047	0.042	0.043	0.030	0.027
0.039	0.035	0.036	0.051	0.040
0.041	0.029	0.030	0.025	0.038
0.040	0.036	0.053	0.053	0.040

e. At depth of 9 mm

0.036	0.024	0.023	0.026	0.025
0.038	0.033	0.032	0.024	0.023
0.032	0.029	0.027	0.042	0.030
0.034	0.020	0.024	0.020	0.031
0.034	0.029	0.045	0.040	0.095

Table 8. **End-on position (Configuration 3).** The SARs measured for the Quantatw Model ZG1S PC with built-in Ambit Model ZG1S 802.11a Antenna for the normal mode at 5.20 GHz (see Fig. 10).

1-g SAR = 0.384 W/kg

a. At depth of 1 mm

0.384	0.611	0.839	0.874	0.720
0.406	0.684	0.903	0.927	0.787
0.452	0.714	0.960	0.930	0.786
0.470	0.735	0.913	0.896	0.765
0.462	0.693	0.865	0.881	0.719

b. At depth of 3 mm

0.276	0.428	0.574	0.596	0.505
0.298	0.478	0.621	0.640	0.554
0.326	0.501	0.642	0.637	0.553
0.340	0.511	0.626	0.617	0.536
0.337	0.487	0.596	0.606	0.512

c. At depth of 5 mm

0.191	0.284	0.367	0.377	0.334
0.212	0.316	0.400	0.414	0.368
0.227	0.332	0.396	0.406	0.370
0.237	0.336	0.401	0.398	0.355
0.238	0.326	0.387	0.392	0.349

d. At depth of 7 mm

0.130	0.180	0.218	0.220	0.208
0.148	0.197	0.239	0.250	0.230
0.154	0.209	0.221	0.238	0.234
0.160	0.209	0.237	0.238	0.223
0.165	0.210	0.238	0.239	0.229

e. At depth of 9 mm

0.092	0.115	0.126	0.123	0.126
0.106	0.121	0.139	0.148	0.139
0.108	0.130	0.118	0.134	0.148
0.111	0.131	0.136	0.139	0.140
0.118	0.139	0.149	0.148	0.154

Table 9. **End-on position (Configuration 3).** The SARs measured for the Quantatw Model ZG1S PC with built-in Ambit Model ZG1S 802.11a Antenna for the normal mode at 5.30 GHz (see Fig. 10).

1-g SAR = 0.424 W/kg

a. At depth of 1 mm

0.625	0.871	0.958	0.843	0.648
0.704	0.935	1.019	0.887	0.689
0.748	0.984	1.061	0.909	0.693
0.743	0.986	1.030	0.871	0.677
0.719	0.940	0.942	0.831	0.607

b. At depth of 3 mm

0.435	0.586	0.644	0.579	0.454
0.480	0.634	0.689	0.608	0.485
0.516	0.666	0.715	0.620	0.485
0.518	0.658	0.695	0.600	0.474
0.506	0.639	0.644	0.575	0.439

c. At depth of 5 mm

0.286	0.364	0.401	0.372	0.301
0.305	0.399	0.429	0.389	0.322
0.333	0.417	0.445	0.395	0.321
0.339	0.404	0.434	0.387	0.314
0.339	0.404	0.412	0.375	0.307

d. At depth of 7 mm

0.178	0.205	0.227	0.222	0.188
0.178	0.228	0.241	0.228	0.201
0.200	0.237	0.250	0.233	0.200
0.207	0.222	0.247	0.231	0.197
0.216	0.237	0.245	0.232	0.208

e. At depth of 9 mm

0.110	0.109	0.123	0.129	0.116
0.100	0.123	0.125	0.127	0.121
0.116	0.126	0.131	0.133	0.122
0.123	0.115	0.135	0.131	0.123
0.139	0.135	0.145	0.144	0.144

Table 10. **End-on position (Configuration 3).** The SARs measured for the Quantatw Model ZG1S PC with built-in Ambit Model ZG1S 802.11a Antenna for the normal mode at 5.745 GHz (see Fig. 10).

1-g SAR = 0.290 W/kg

a. At depth of 1 mm

0.564	0.590	0.541	0.472	0.376
0.586	0.643	0.581	0.516	0.395
0.592	0.669	0.624	0.529	0.417
0.587	0.673	0.660	0.540	0.414
0.556	0.614	0.621	0.517	0.424

b. At depth of 3 mm

0.383	0.407	0.383	0.332	0.275
0.397	0.441	0.404	0.366	0.287
0.402	0.454	0.431	0.380	0.304
0.399	0.460	0.450	0.382	0.313
0.384	0.424	0.432	0.377	0.323

c. At depth of 5 mm

0.243	0.263	0.257	0.222	0.195
0.250	0.283	0.265	0.246	0.202
0.256	0.287	0.281	0.260	0.213
0.253	0.294	0.287	0.258	0.230
0.251	0.276	0.285	0.265	0.242

d. At depth of 7 mm

0.142	0.159	0.165	0.142	0.137
0.146	0.169	0.164	0.157	0.137
0.152	0.168	0.174	0.170	0.143
0.150	0.174	0.171	0.166	0.165
0.156	0.170	0.181	0.183	0.181

e. At depth of 9 mm

0.080	0.095	0.105	0.091	0.101
0.085	0.099	0.102	0.099	0.095
0.090	0.096	0.110	0.111	0.096
0.090	0.101	0.103	0.107	0.118
0.098	0.106	0.120	0.130	0.139

Table 11. **Edge-on position (Configuration 2).** The SARs measured for the Compal Model L1S PC with built-in Ambit Model BY27 802.11a Antenna for the normal mode at 5.20 GHz (see Fig. 9).

1-g SAR = 0.233 W/kg

a. At depth of 1 mm

0.337	0.356	0.378	0.355	0.357
0.360	0.374	0.407	0.379	0.378
0.373	0.384	0.415	0.397	0.380
0.385	0.392	0.418	0.429	0.415
0.401	0.418	0.440	0.432	0.427

b. At depth of 3 mm

0.254	0.268	0.280	0.266	0.263
0.268	0.278	0.300	0.287	0.278
0.282	0.286	0.306	0.296	0.281
0.289	0.295	0.310	0.314	0.303
0.302	0.317	0.328	0.329	0.321

c. At depth of 5 mm

0.187	0.199	0.203	0.195	0.189
0.195	0.201	0.215	0.212	0.198
0.207	0.207	0.218	0.214	0.202
0.211	0.216	0.224	0.223	0.214
0.223	0.235	0.239	0.247	0.223

d. At depth of 7 mm

0.137	0.147	0.144	0.140	0.133
0.139	0.145	0.153	0.155	0.138
0.149	0.148	0.151	0.151	0.144
0.152	0.156	0.161	0.156	0.148
0.164	0.173	0.174	0.187	0.134

e. At depth of 9 mm

0.104	0.114	0.106	0.104	0.096
0.102	0.109	0.113	0.117	0.098
0.107	0.109	0.105	0.107	0.106
0.110	0.115	0.120	0.114	0.106
0.127	0.130	0.134	0.147	0.124

Table 12. **Edge-on position (Configuration 2).** The SARs measured for the Compal Model L1S PC with built-in Ambit Model BY27 802.11a Antenna for the normal mode at 5.30 GHz (see Fig. 9).

1-g SAR = 0.306 W/kg

a. At depth of 1 mm

0.511	0.505	0.533	0.510	0.487
0.539	0.557	0.564	0.570	0.538
0.542	0.571	0.581	0.576	0.532
0.539	0.576	0.587	0.568	0.550
0.529	0.559	0.590	0.582	0.553

b. At depth of 3 mm

0.366	0.362	0.381	0.371	0.352
0.383	0.399	0.405	0.402	0.388
0.392	0.409	0.413	0.410	0.387
0.393	0.413	0.418	0.409	0.395
0.388	0.403	0.431	0.428	0.408

c. At depth of 5 mm

0.251	0.247	0.260	0.261	0.245
0.259	0.273	0.278	0.270	0.267
0.273	0.279	0.280	0.279	0.272
0.276	0.285	0.284	0.283	0.274
0.276	0.281	0.305	0.305	0.294

d. At depth of 7 mm

0.165	0.162	0.171	0.178	0.165
0.169	0.180	0.183	0.175	0.176
0.183	0.182	0.183	0.184	0.185
0.189	0.191	0.186	0.191	0.186
0.192	0.192	0.213	0.214	0.210

e. At depth of 9 mm

0.110	0.106	0.113	0.123	0.111
0.111	0.121	0.121	0.117	0.115
0.123	0.116	0.123	0.124	0.128
0.131	0.131	0.124	0.131	0.130
0.136	0.137	0.153	0.154	0.157

Table 13. **Edge-on position (Configuration 2).** The SARs measured for the Compal Model L1S PC with built-in Ambit Model BY27 802.11a Antenna for the normal mode at 5.745 GHz (see Fig. 9).

1-g SAR = 0.352 W/kg

a. At depth of 1 mm

0.608	0.610	0.664	0.655	0.630
0.634	0.686	0.692	0.681	0.657
0.673	0.727	0.723	0.718	0.662
0.709	0.708	0.733	0.762	0.714
0.708	0.731	0.742	0.728	0.716

b. At depth of 3 mm

0.424	0.419	0.450	0.450	0.433
0.435	0.466	0.471	0.471	0.453
0.462	0.495	0.494	0.491	0.461
0.483	0.490	0.507	0.517	0.491
0.486	0.507	0.517	0.510	0.509

c. At depth of 5 mm

0.278	0.271	0.283	0.287	0.276
0.278	0.292	0.298	0.304	0.291
0.295	0.312	0.314	0.313	0.300
0.306	0.317	0.328	0.326	0.317
0.313	0.330	0.341	0.338	0.347

d. At depth of 7 mm

0.170	0.163	0.162	0.169	0.161
0.162	0.166	0.171	0.181	0.173
0.174	0.179	0.181	0.182	0.181
0.177	0.190	0.198	0.187	0.190
0.188	0.202	0.212	0.214	0.230

e. At depth of 9 mm

0.101	0.096	0.088	0.093	0.087
0.087	0.087	0.092	0.101	0.097
0.098	0.095	0.096	0.099	0.103
0.097	0.109	0.115	0.102	0.112
0.110	0.121	0.132	0.137	0.157

Table 14. The peak 1-g SARs measured for the Quantatw Model ZG1S PC with built-in Ambit Model ZG1S 802.11a Antenna.

		1-g SAR in W/kg		
PC position relative to the flat phantom	Spacing to the bottom of the phantom	5.20 GHz normal mode	5.30 GHz normal mode	5.745 GHz normal mode
Configuration 1 – "**Above-lap"** position (see Fig. 4); bottom of PC pressed against bottom of the flat phantom	0 cm	0.114	0.084	0.057
Configuration 2 – **"Edge-on"** position (see Fig. 7); antenna edge (right edge) of PC pressed against bottom of the flat phantom	0 cm	<0.02*	<0.02*	<0.02*
Configuration 3 – "End-on" position (see Fig. 10); broader back edge of PC pressed against bottom of the flat phantom	0 cm	0.384	0.424	0.290

* Too low to measure, within the noise limit of the SAR measurement system.

Table 15. The peak 1-g SARs measured for the Quantatw Model ZI1S PC with built-in Ambit Model ZI1S 802.11a Antenna.

		1-g SAR in W/kg		
PC position relative to the flat phantom	Spacing to the bottom of the phantom	5.20 GHz normal mode	5.30 GHz normal mode	5.745 GHz normal mode
Configuration 1 – **"Above-lap"** position (see Fig. 4); bottom of PC pressed against bottom of the flat phantom	0 cm	<0.02*	<0.02*	<0.02*
Configuration 2 – **"Edge-on"** position (see Fig. 8); antenna edge (right edge) of PC pressed against bottom of the flat phantom	0 cm	<0.02*	<0.02*	<0.02*
Configuration 3 – "End-on" position (see Fig. 11); broader back edge of PC pressed against bottom of the flat phantom	0 cm	<0.02*	<0.02*	<0.02*

* Too low to measure, within the noise limit of the SAR measurement system.

Table 16. The peak 1-g SARs measured for the Compal Model L1S PC with built-in Ambit Model BY27 802.11a Antenna.

		1-g SAR in W/kg		
PC position relative to the flat phantom	Spacing to the bottom of the phantom	5.20 GHz normal mode	5.30 GHz normal mode	5.745 GHz normal mode
Configuration 1 – "Above-lap" position (see Fig. 4); bottom of PC pressed against bottom of the flat phantom	0 cm	<0.02*	<0.02*	<0.02*
Configuration 2 – "Edge-on" position (see Fig. 9); antenna edge (right edge) of PC parallel to the bottom of the flat phantom	1.5 cm	0.233	0.306	0.352
Configuration 3 – "End-on" position (see Fig. 12); broader back edge of PC pressed against bottom of the flat phantom	0 cm	<0.02*	<0.02*	<0.02*

* Too low to measure, within the noise limit of the SAR measurement system.

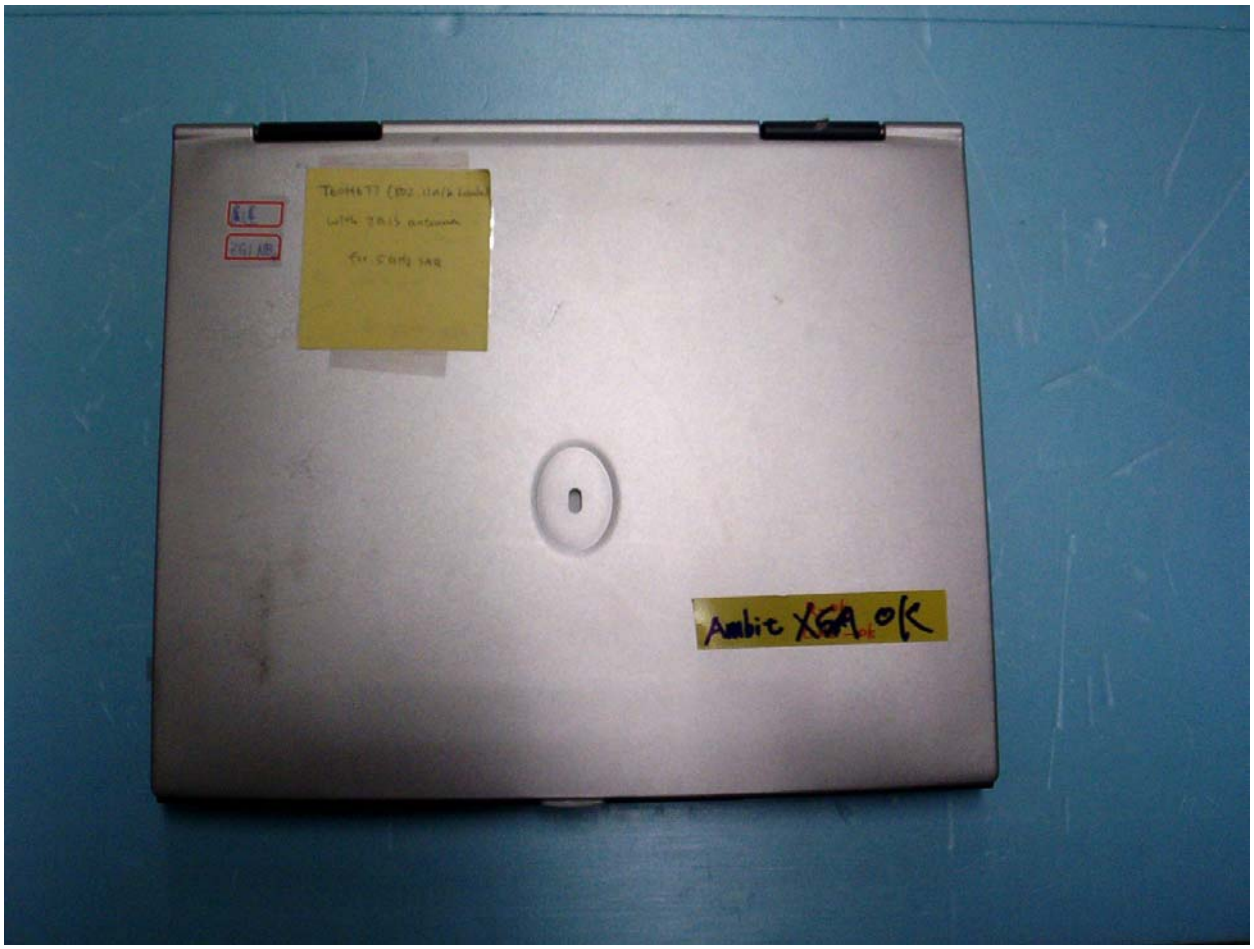

a. Top cover closed.

Fig. 1. Photograph of the Quantatw Model ZG1S PC with built-in Ambit Microsystems Model ZG1S 802.11a Wireless Antenna.

b. View from the bottom side of the laptop computer.

Fig. 1. Photograph of the Quantatw Model ZG1S PC with built-in Ambit Microsystems Model ZG1S 802.11a Wireless Antenna.

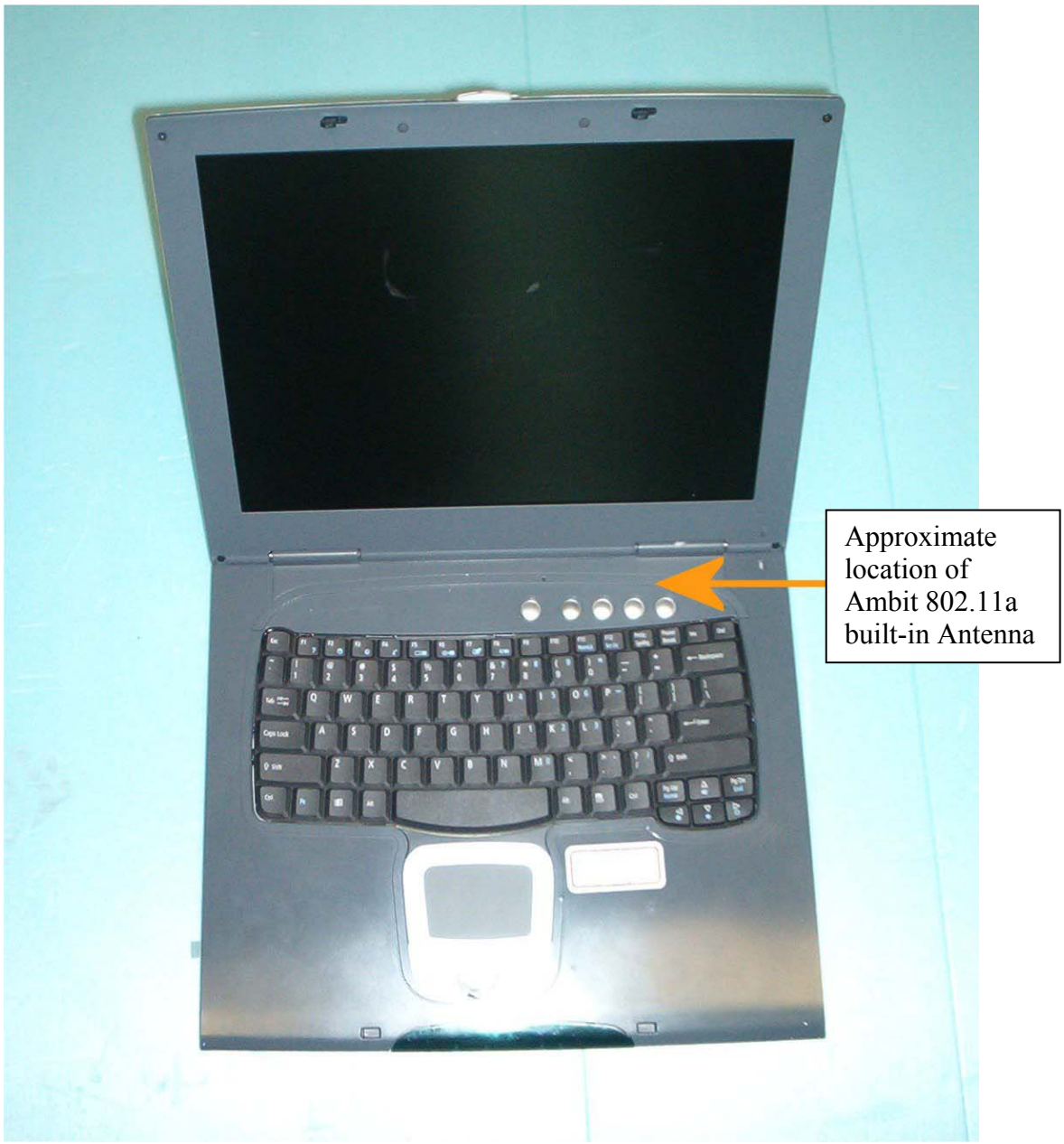

c. Top cover with screen open.

Fig. 1. Photograph of the Quantatw Model ZG1S PC with built-in Ambit Microsystems Model ZG1S 802.11a Wireless Antenna.

a. Top cover closed.

Fig. 2. Photograph of the Quantatw Model ZI1S PC with built-in Ambit Microsystems Model ZI1S 802.11a Wireless Antenna.

b. View from the bottom side of the laptop computer.

Fig. 2. Photograph of the Quantatw Model ZI1S PC with built-in Ambit Microsystems Model ZI1S 802.11a Wireless Antenna.

c. Top cover with screen open.

Fig. 2. Photograph of the Quantatw Model ZI1S PC with built-in Ambit Microsystems Model ZI1S 802.11a Wireless Antenna.

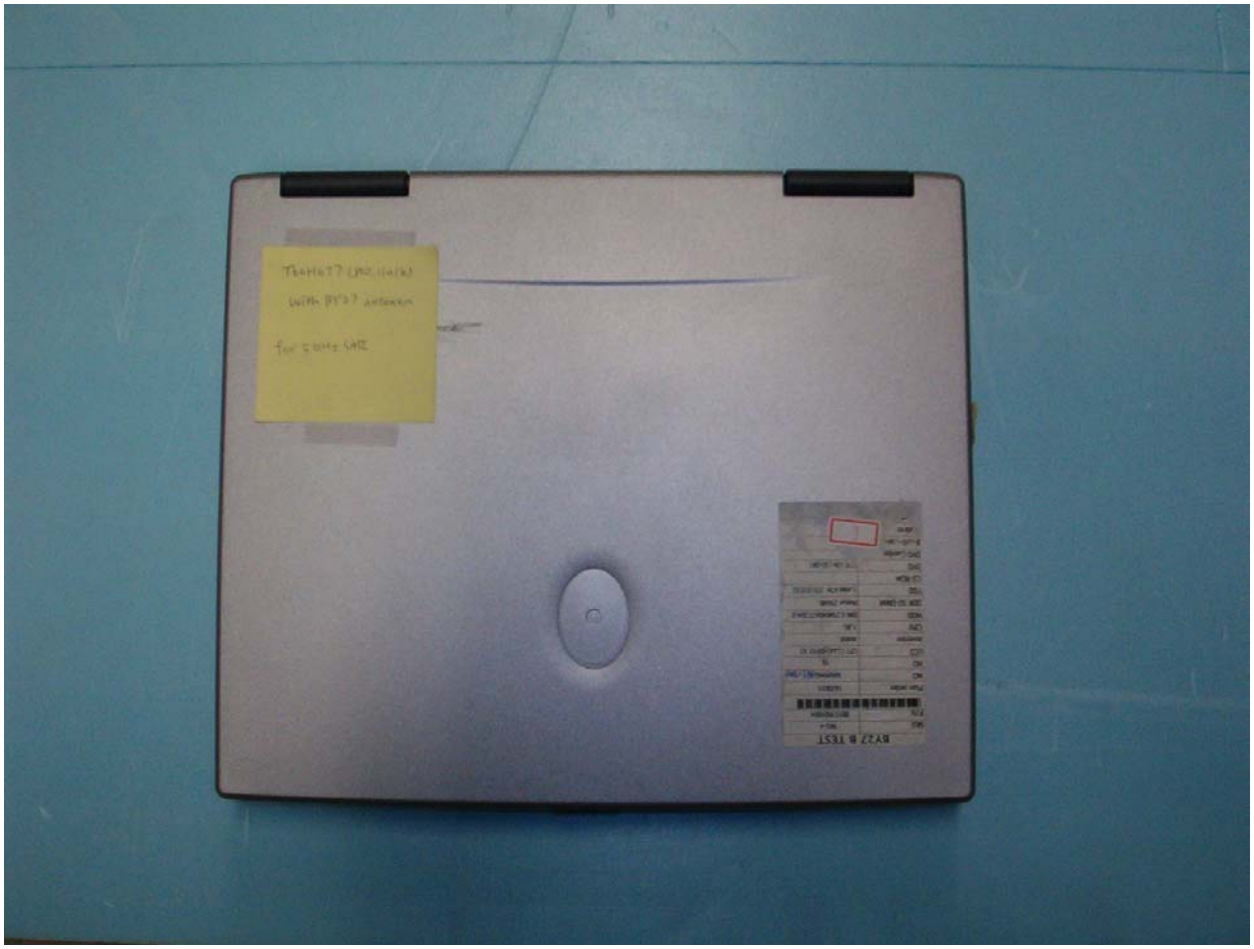

a. Top cover closed.

Fig. 3. Photograph of the Compal Model L1S PC with built-in Ambit Microsystems Model BY27 802.11a Wireless Antenna.

b. View from the bottom side of the laptop computer.

Fig. 3. Photograph of the Compal Model L1S PC with built-in Ambit Microsystems Model BY27 802.11a Wireless Antenna.

c. Top cover with screen open.

Fig. 3. Photograph of the Compal Model L1S PC with built-in Ambit Microsystems Model BY27 802.11a Wireless Antenna.

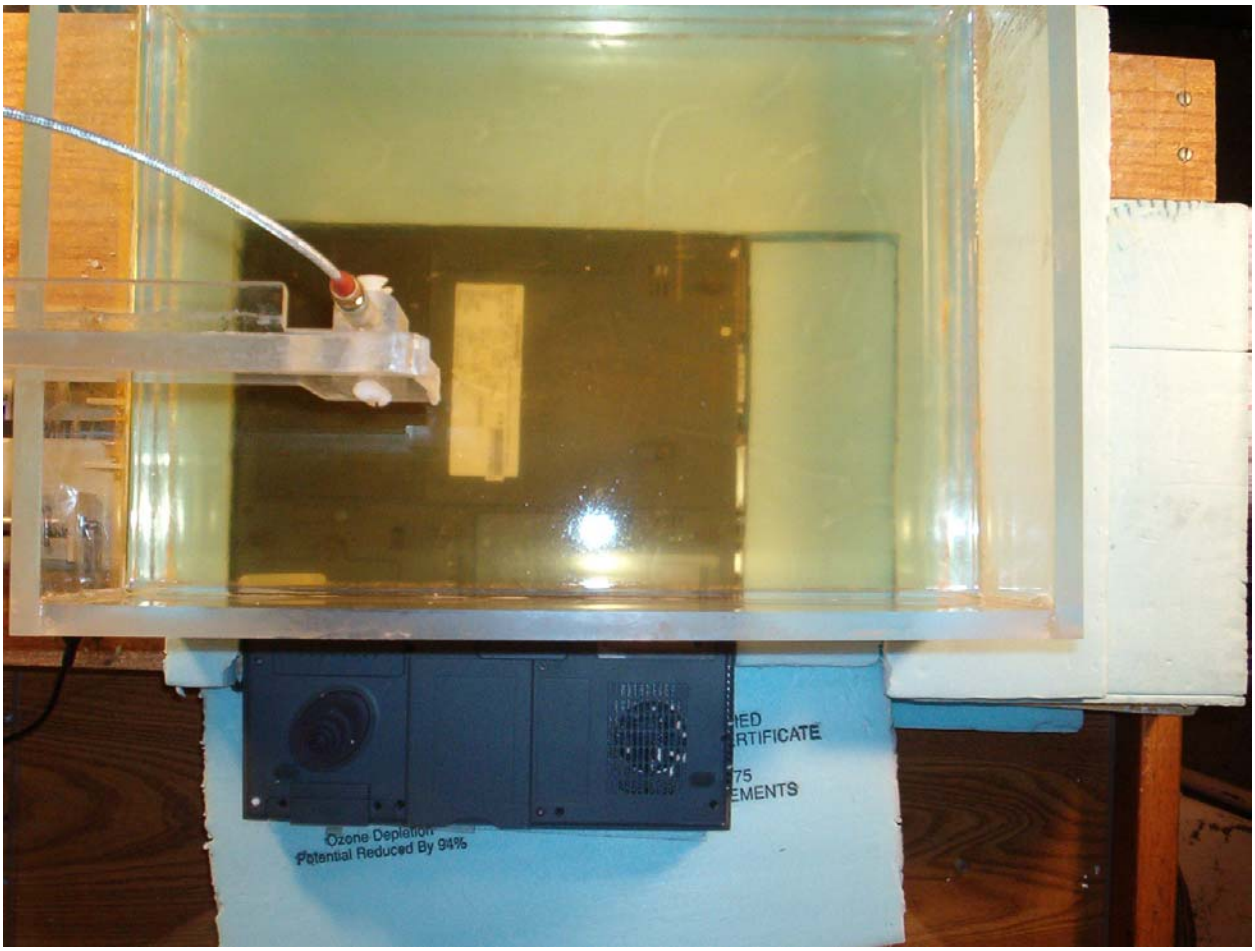

Fig. 4. Photograph of the bottom of Quantatw Model ZG1S PC pressed against the base of the planar phantom. This is **Configuration 1** for SAR testing. This Configuration 1 was also used for Quantatw Model ZI1S and Compal Model L1S PCs with the bottom of each of the PCs pressed against the base of the planar phantom.

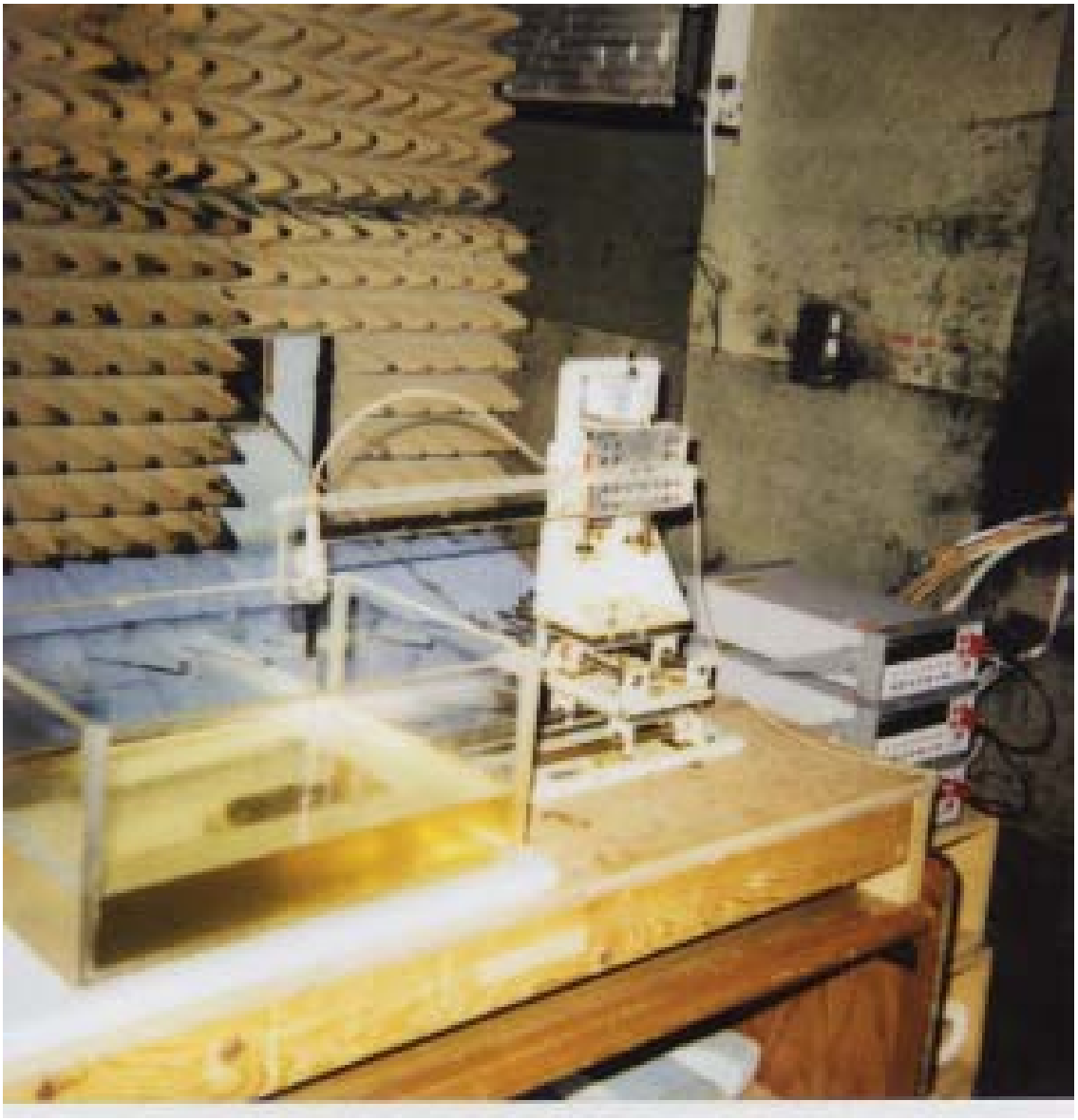

Fig. 5. Photograph of the three-dimensional stepper-motor-controlled SAR measurement system using a planar phantom (see Figs. 4, and 7-12 for a detailed placement of the various PCs relative to this phantom).

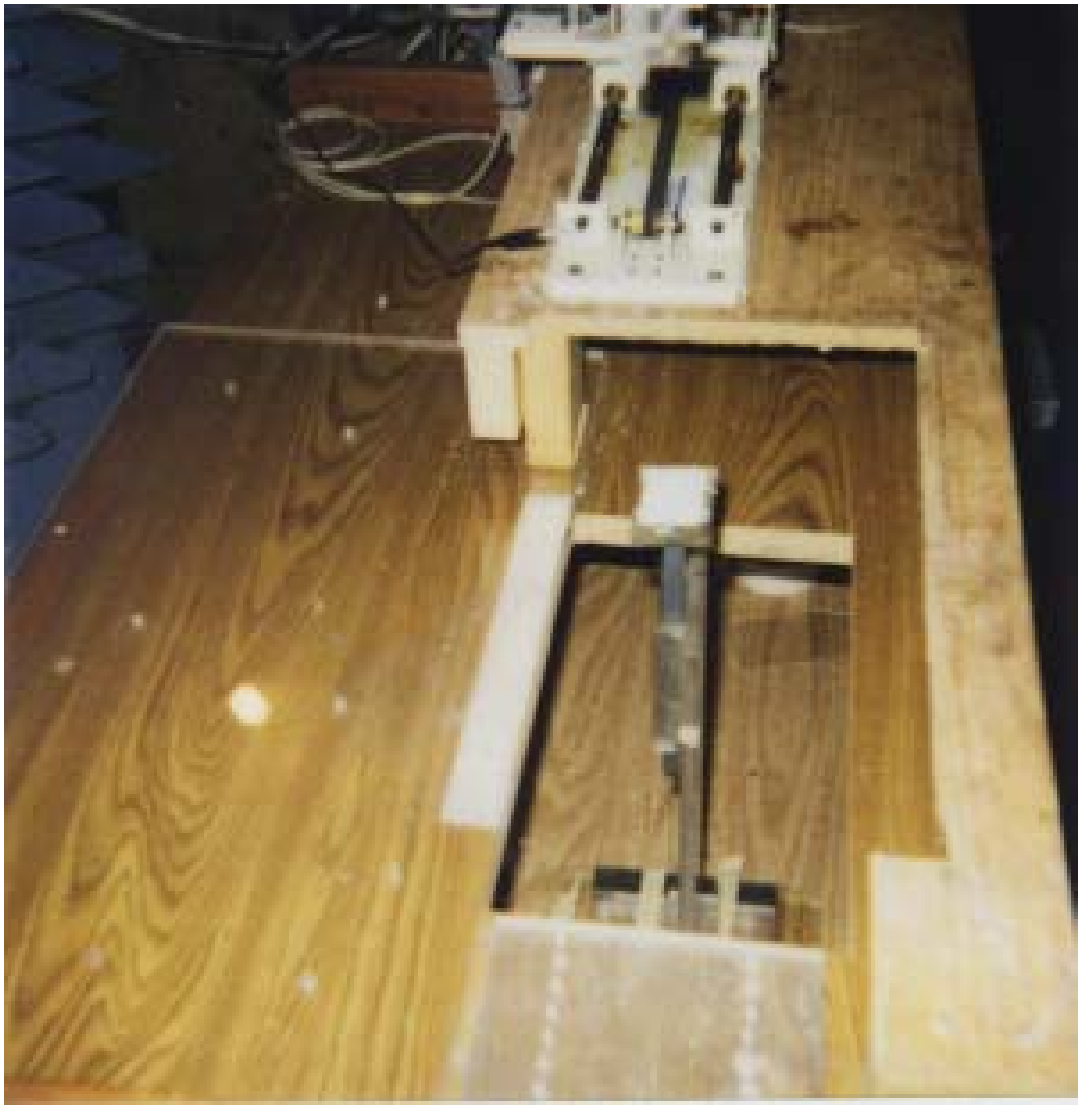

Fig. 6. The plastic holder used to support the portable PCs against the planar phantom.

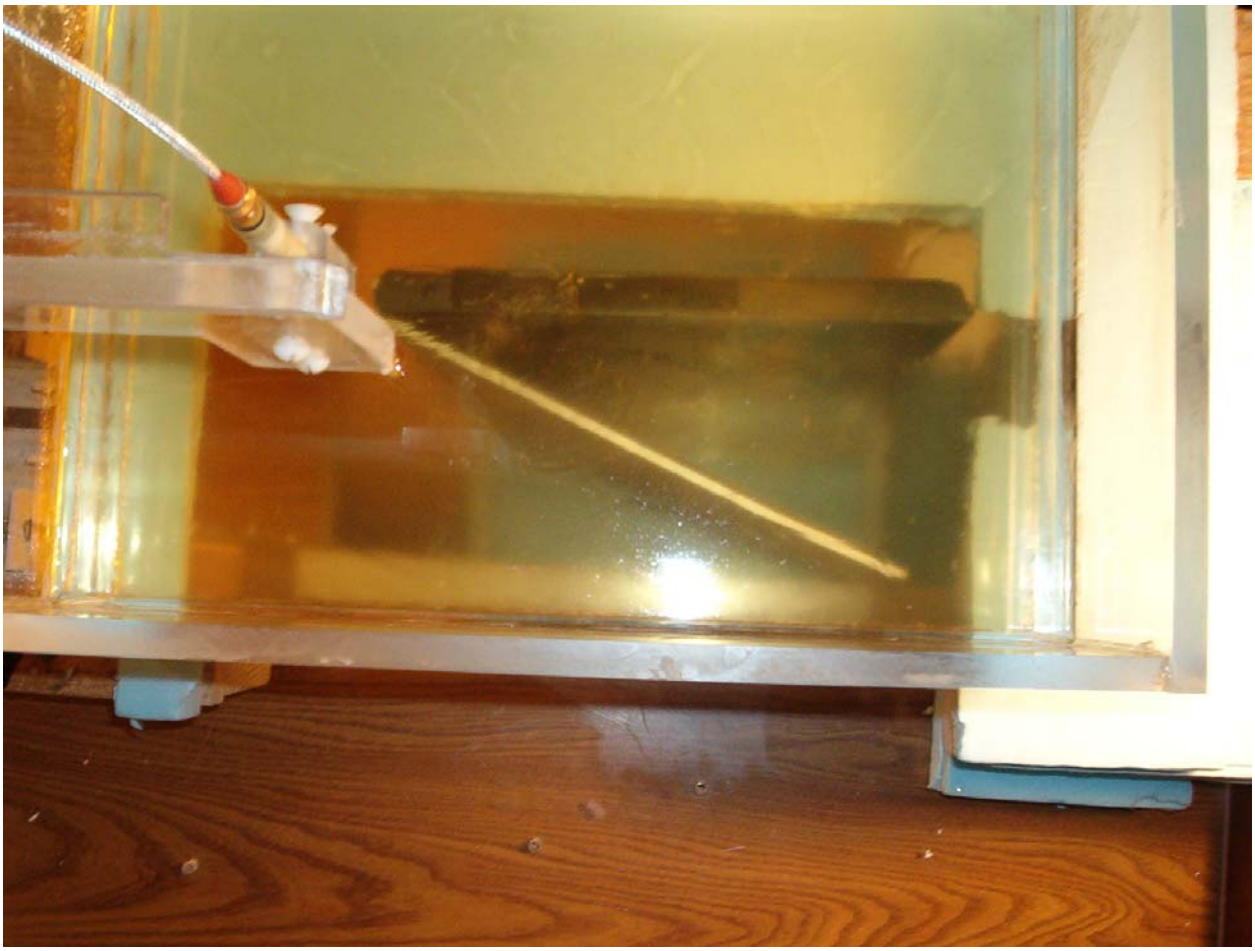

a. View from the top of the planar phantom.

Fig. 7. Photograph of the Quantatw Model ZG1S PC with the screen partially open and the antenna edge (right edge) at 90° pressed against the bottom of the planar phantom with separation of 0 cm. This is **Configuration 2** for SAR testing and represents the case of a bystander standing to the right of the PC with a separation of 0 cm from the antenna side of the laptop computer.

b. Side view.

Fig. 7. Photograph of the Quantatw Model ZG1S PC with the screen partially open and the antenna edge (right edge) at 90° pressed against the bottom of the planar phantom with separation of 0 cm. This is **Configuration 2** for SAR testing and represents the case of a bystander standing to the right of the PC with a separation of 0 cm from the antenna side of the laptop computer.

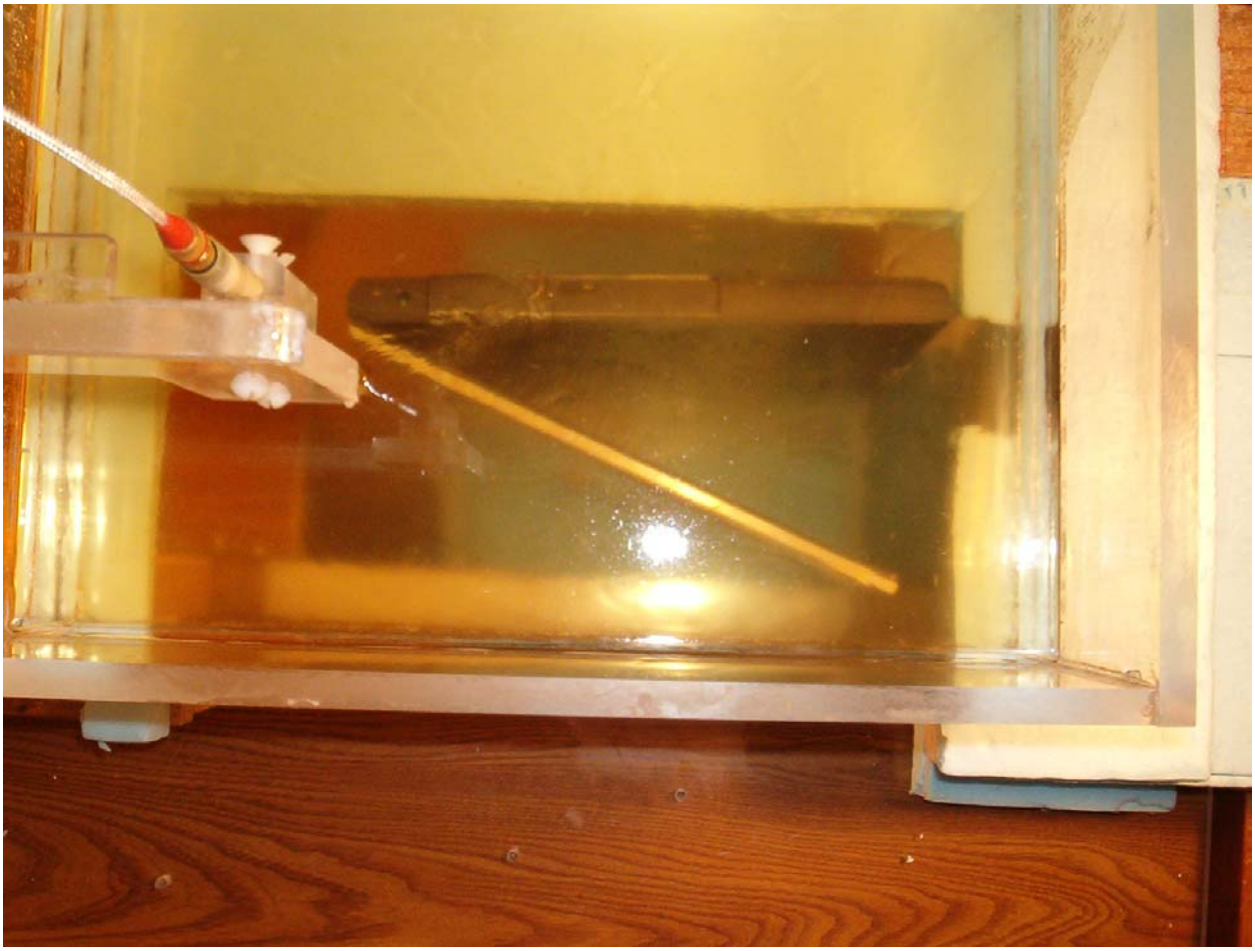

a. View from the top of the planar phantom.

Fig. 8. Photograph of the Quantatw Model ZI1S PC with the screen partially open and the antenna edge (right edge) at 90° pressed against the bottom of the planar phantom with separation of 0 cm. This is **Configuration 2** for SAR testing and represents the case of a bystander standing to the right of the PC with a separation of 0 cm from the antenna side of the laptop computer.

b. Side view.

Fig. 8. Photograph of the Quantatw Model ZI1S PC with the screen partially open and the antenna edge (right edge) at 90° pressed against the bottom of the planar phantom with separation of 0 cm. This is **Configuration 2** for SAR testing and represents the case of a bystander standing to the right of the PC with a separation of 0 cm from the antenna side of the laptop computer.

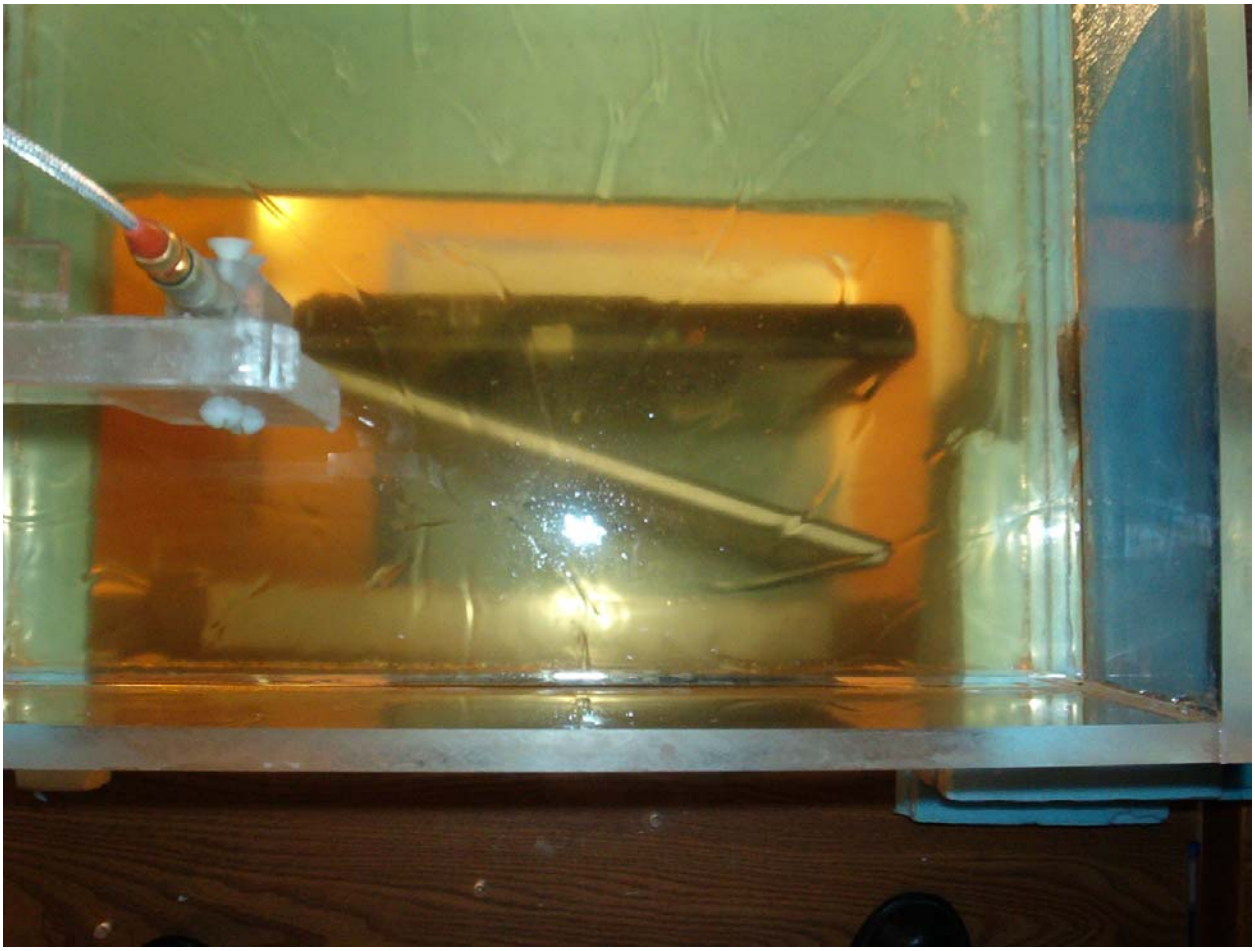

a. View from the top of the planar phantom.

Fig. 9. Photograph of the Compal Model L1S PC with the screen partially open and the antenna edge at 90° parallel to the base of the planar phantom with a separation of 1.5 cm. This is **Configuration 2** for SAR testing and represents the case of a bystander standing to the right of the PC with a separation of 1.5 cm from the antenna edge of the laptop computer.

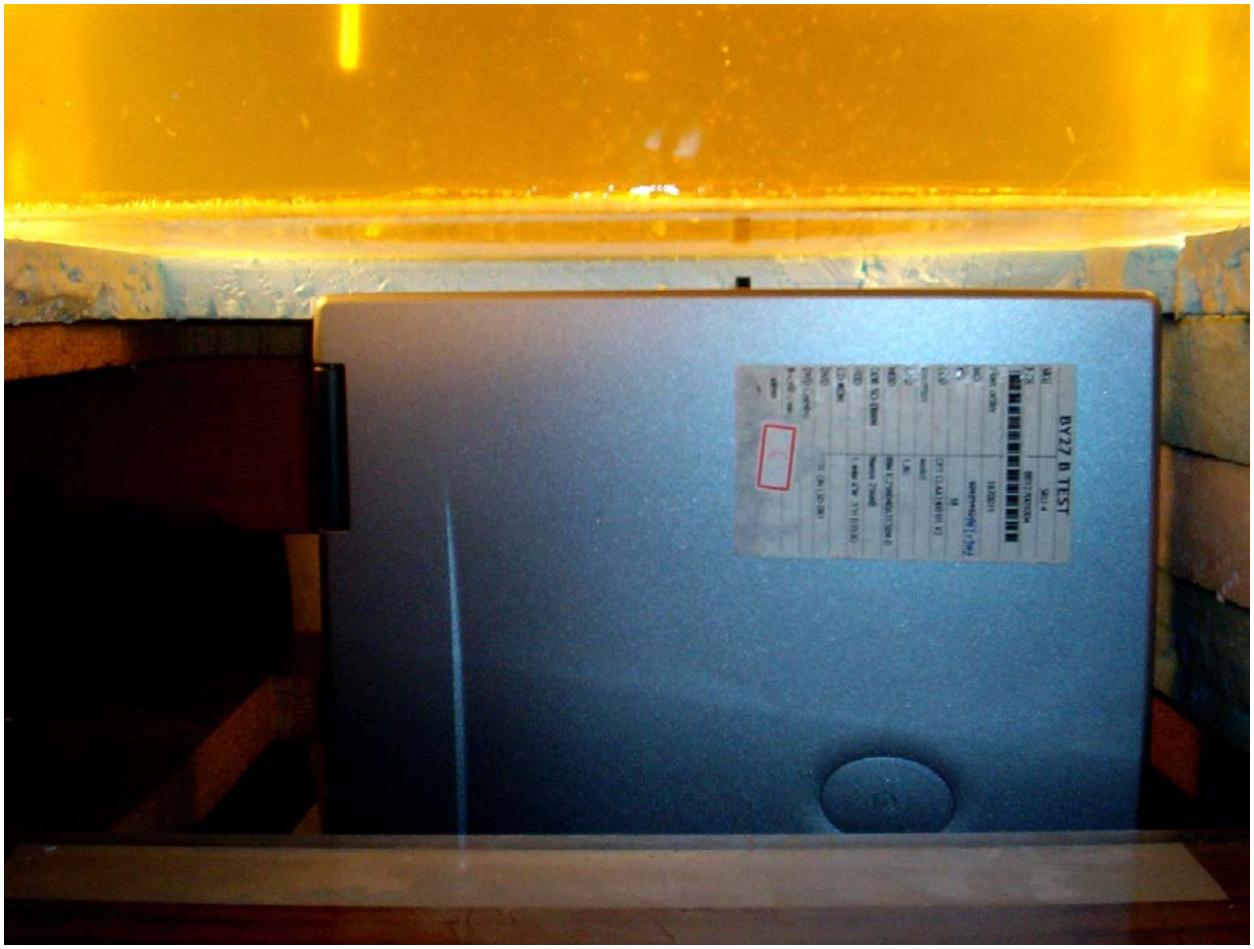

b. Side view.

Fig. 9. Photograph of the Compal Model L1S PC with the screen partially open and the antenna edge at 90° parallel to the base of the planar phantom with a separation of 1.5 cm. This is **Configuration 2** for SAR testing and represents the case of a bystander standing to the right of the PC with a separation of 1.5 cm from the antenna edge of the laptop computer.

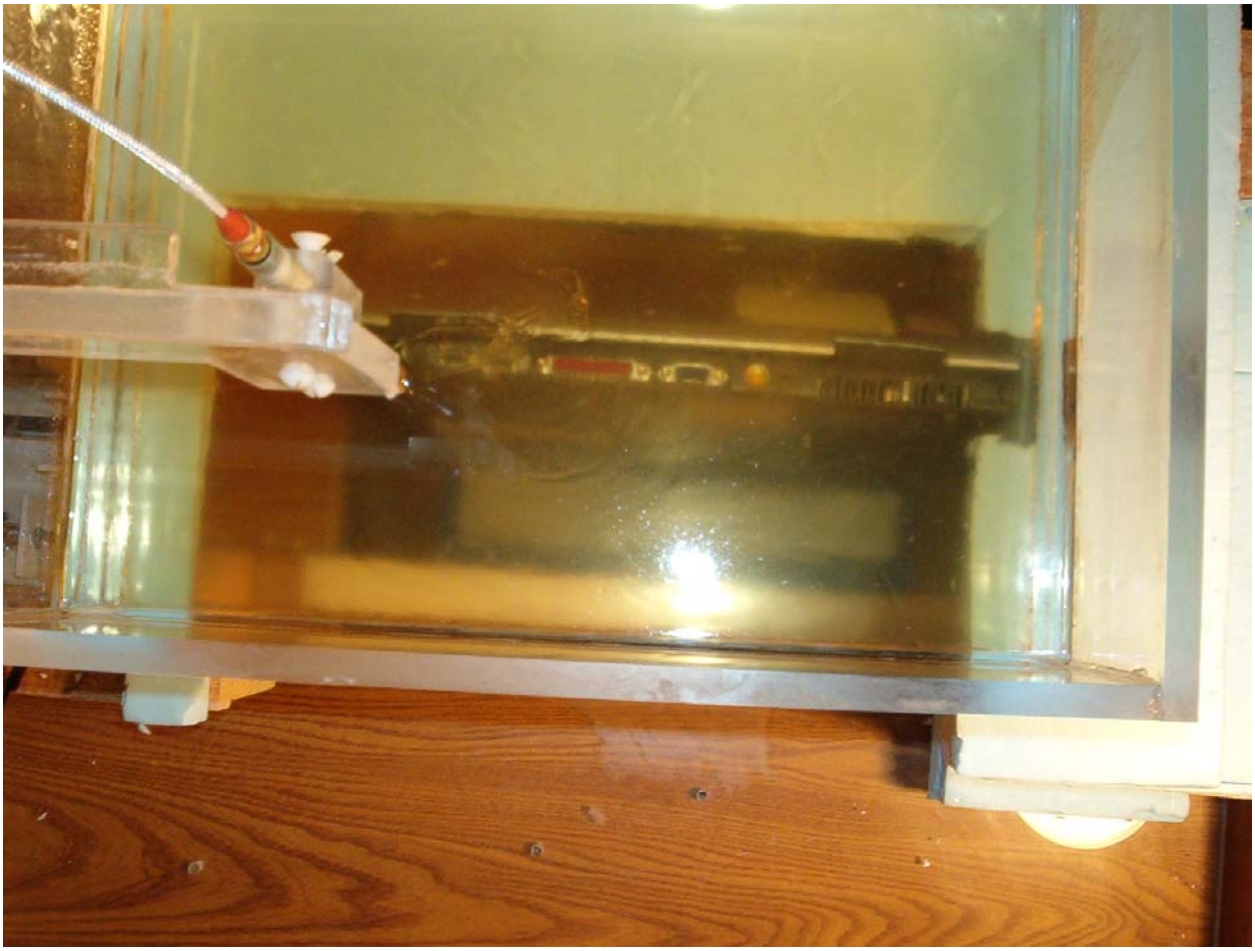

a. View from the top of the planar phantom.

Fig. 10. Photograph of the Quantatw ZG1S PC with the screen partially open and the broader back edge of the PC at 90° pressed against the bottom of the planar phantom with separation of 0 cm. This is **Configuration 3** for SAR testing and represents the case of a bystander behind the PC screen with a separation of 0 cm.

b. Side view.

Fig. 10. Photograph of the Quantatw ZG1S PC with the screen partially open and the broader back edge of the PC at 90° pressed against the bottom of the planar phantom with separation of 0 cm. This is **Configuration 3** for SAR testing and represents the case of a bystander behind the PC screen with a separation of 0 cm.

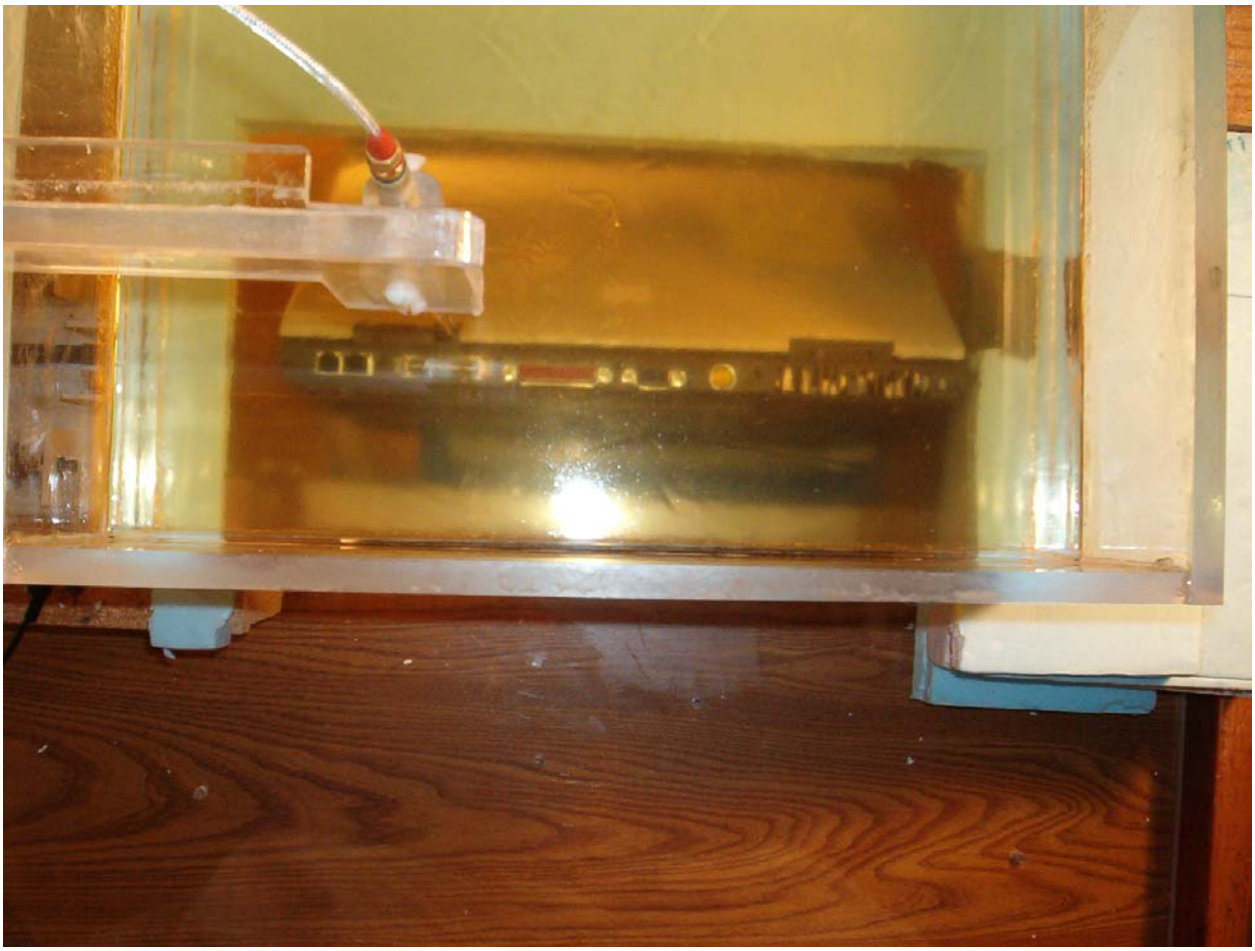

a. View from the top of the planar phantom.

Fig. 11. Photograph of the Quantatw ZI1S PC with the screen partially open and the broader back edge of the PC at 90° pressed against the bottom of the planar phantom with separation of 0 cm. This is **Configuration 3** for SAR testing and represents the case of a bystander behind the PC screen with a separation of 0 cm.

b. Side view.

Fig. 11. Photograph of the Quantatw ZI1S PC with the screen partially open and the broader back edge of the PC at 90° pressed against the bottom of the planar phantom with separation of 0 cm. This is **Configuration 3** for SAR testing and represents the case of a bystander behind the PC screen with a separation of 0 cm.

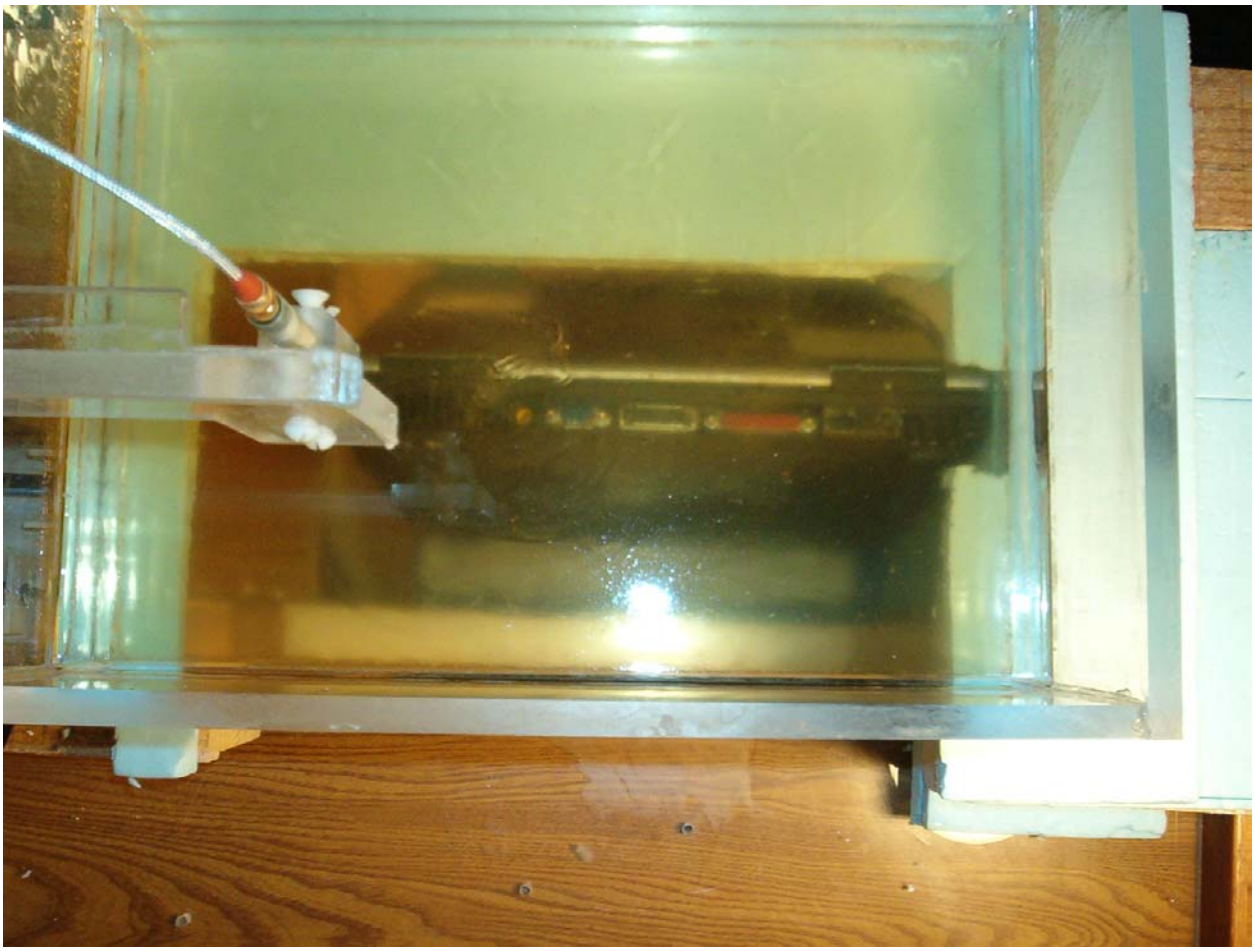

a. View from the top of the planar phantom.

Fig. 12. Photograph of the Compal Model L1S PC with the screen partially open and the broader back edge of the PC at 90° pressed against the bottom of the planar phantom with separation of 0 cm. This is **Configuration 3** for SAR testing and represents the case of a bystander behind the PC screen with a separation of 0 cm.

b. Side view.

Fig. 12. Photograph of the Compal Model L1S PC with the screen partially open and the broader back edge of the PC at 90° pressed against the bottom of the planar phantom with separation of 0 cm. This is **Configuration 3** for SAR testing and represents the case of a bystander behind the PC screen with a separation of 0 cm.

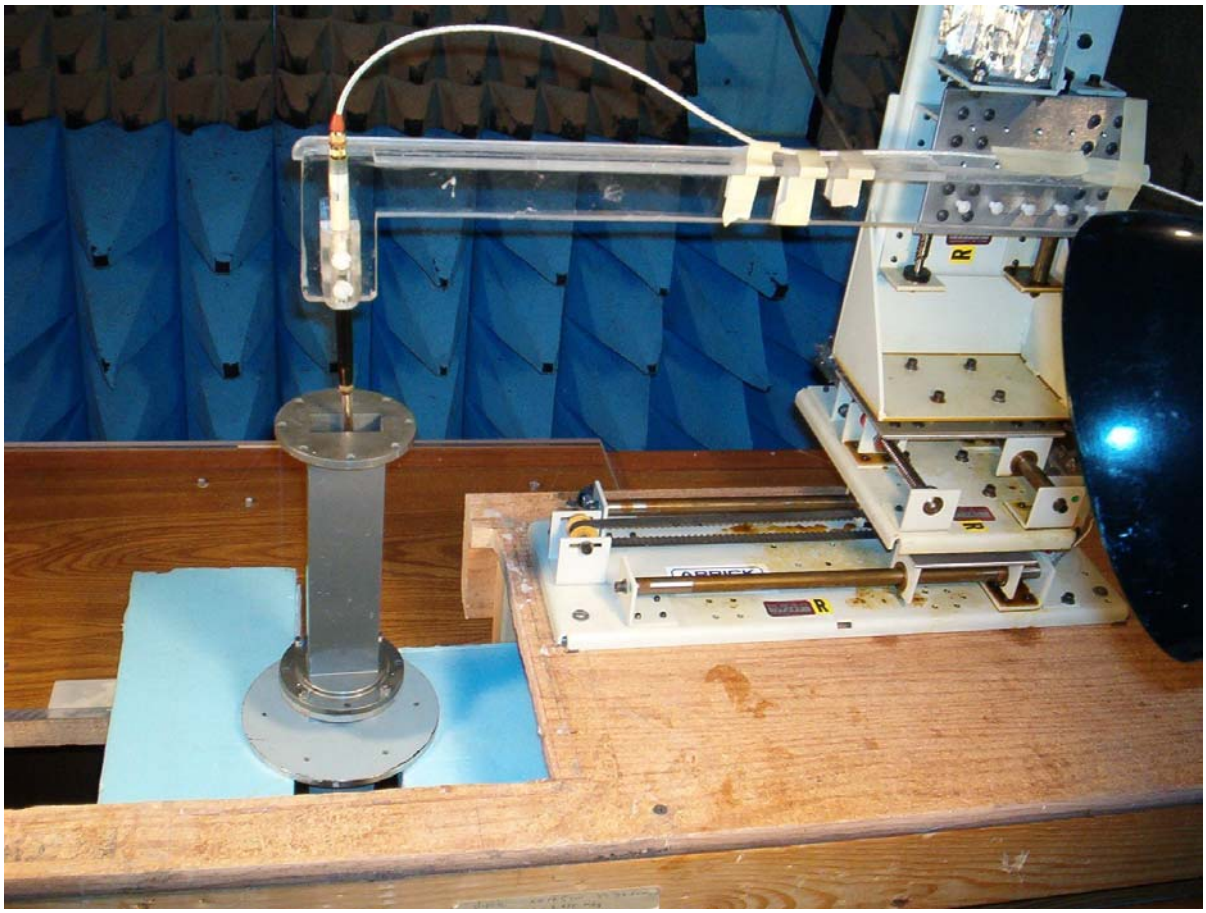

Fig. 13a. A photograph of the waveguide setup used for calibration of the Narda Model 8021 E-field probe in the frequency band 5.2-5.8 GHz.

Fig. 13b. Photograph of the waveguide setup showing also the coax to waveguide coupler at the bottom used to feed power to the vertical waveguide containing the tissue-simulant fluid.

Fig. 14. Photograph of the Narda Model 8021 Broadband Electric Field Probe used for SAR measurements.

Fig. 15. Photograph of the half-wave dipole at 1900 MHz used for system verification.

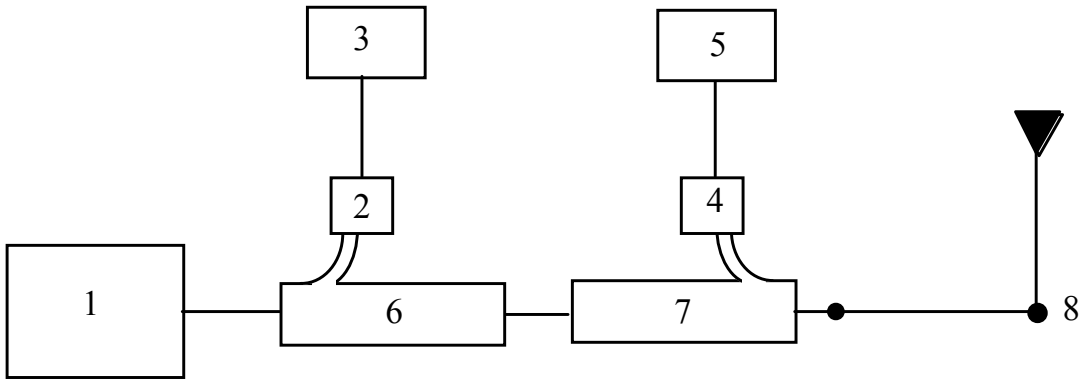

1. RF generator, MCL Model 15222 with Model 6051 plug-in (1000-2000 MHz).
2. HP Model 8481A power sensor.
3. HP Model 436A power meter.
4. HP Model 8482A power sensor.
5. HP Model 436A power meter.
6. Narda Model 3042B-30, 30 dB coaxial directional coupler.
7. Narda Model 3042-10, 10 dB coaxial directional coupler.
8. Reference dipole antenna.

Fig. 16. The microwave circuit arrangement used for SAR system verification.

Fig. 17. Photograph of the Hewlett Packard Model 85070B Dielectric Probe. This is an open-circuited coaxial line probe.

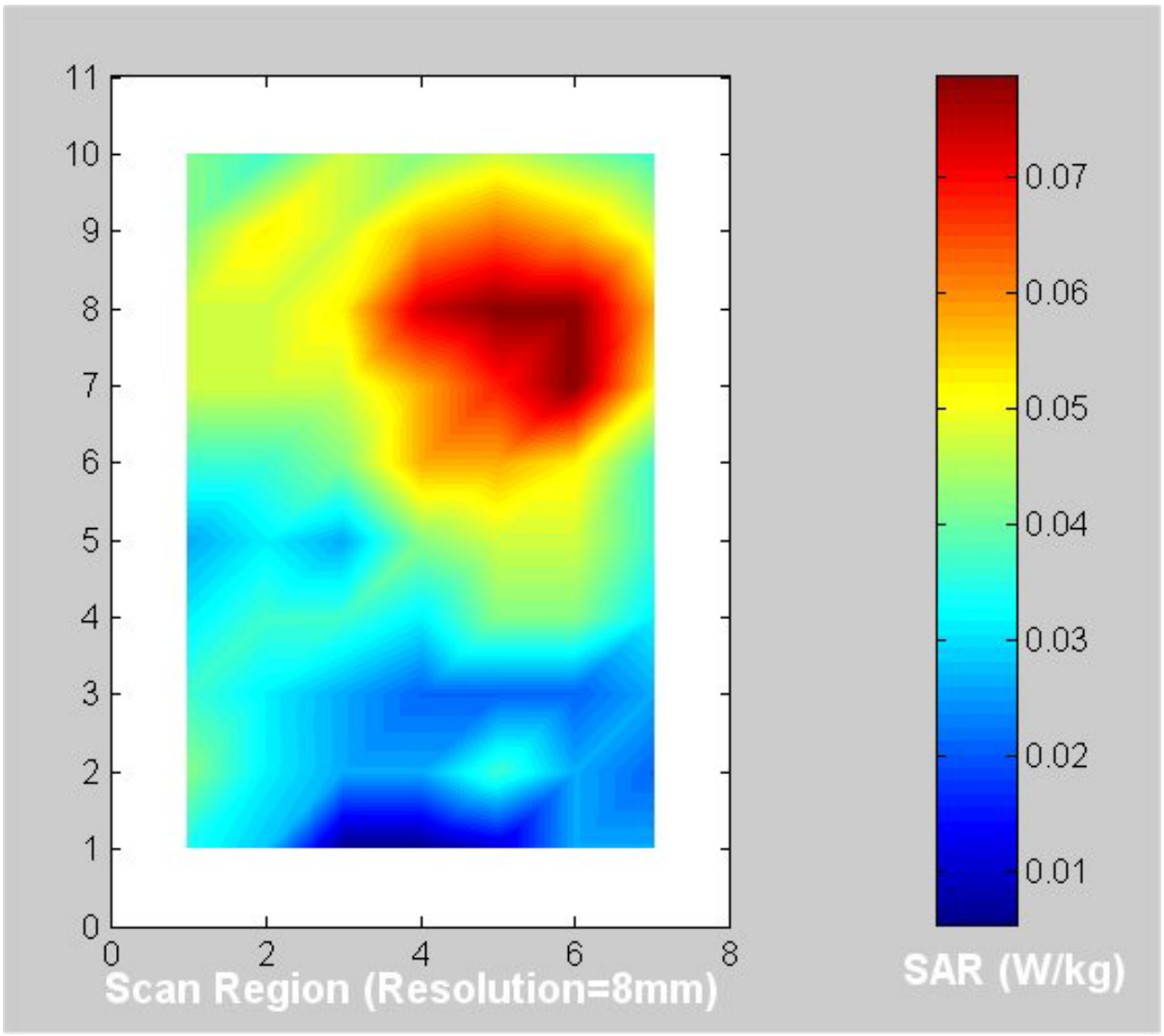

a. 5.20 GHz normal mode (see Table 5 for the peak 1-g SAR).

Fig. 18. Coarse scans for the SAR measurements for the **Above-lap** Configuration 1 of the Quantatw Model ZG1S PC with Ambit Model ZG1S 802.11a antenna. As shown in Fig. 4, the bottom of the Quantatw Model ZG1S PC is pressed against the base of the planar phantom for these measurements.

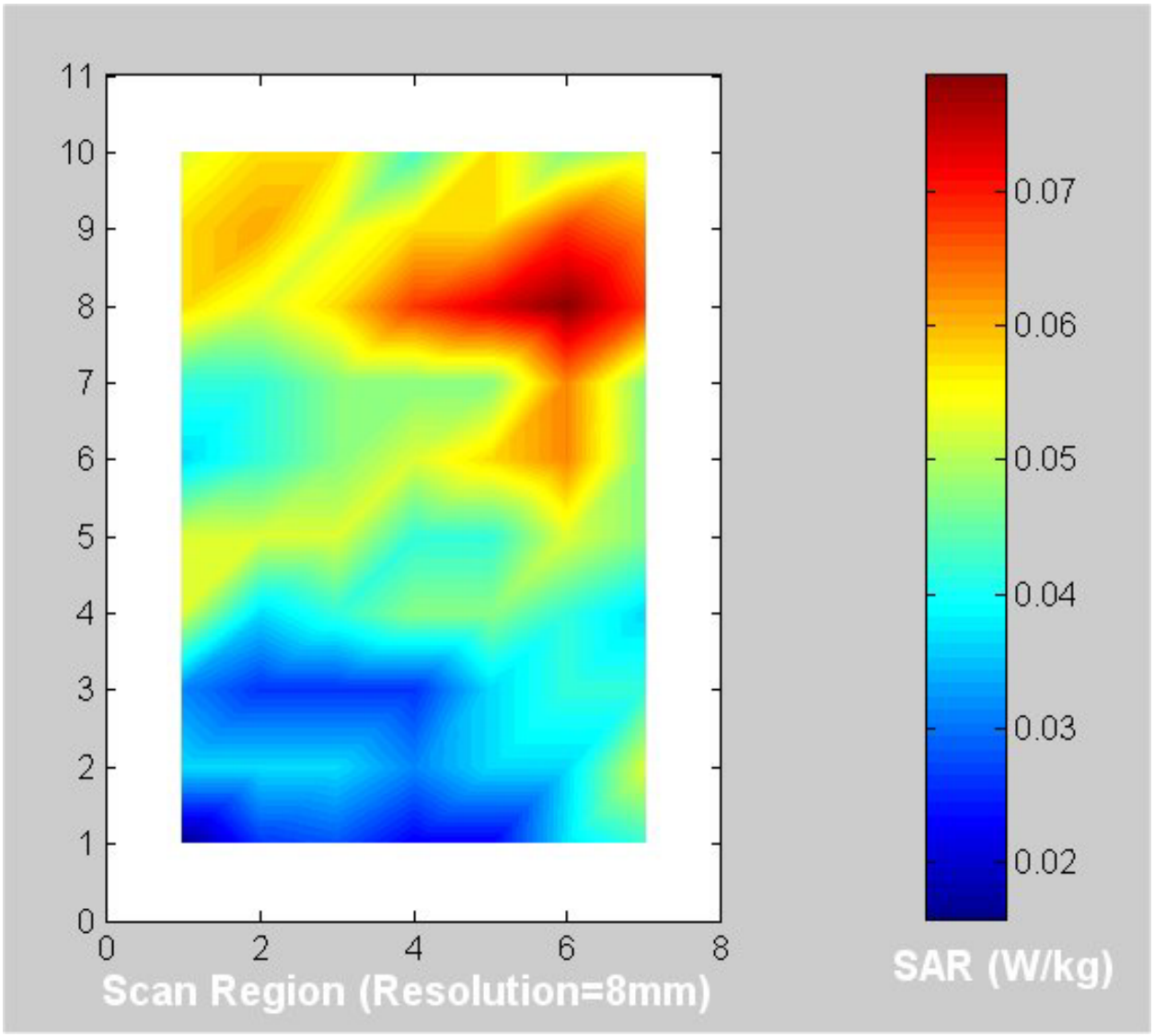

b. 5.30 GHz normal mode (see Table 6 for the peak 1-g SAR).

Fig. 18. Coarse scans for the SAR measurements for the **Above-lap** Configuration 1 of the Quantatw Model ZG1S PC with Ambit Model ZG1S 802.11a antenna. As shown in Fig. 4, the bottom of the Quantatw Model ZG1S PC is pressed against the base of the planar phantom for these measurements.

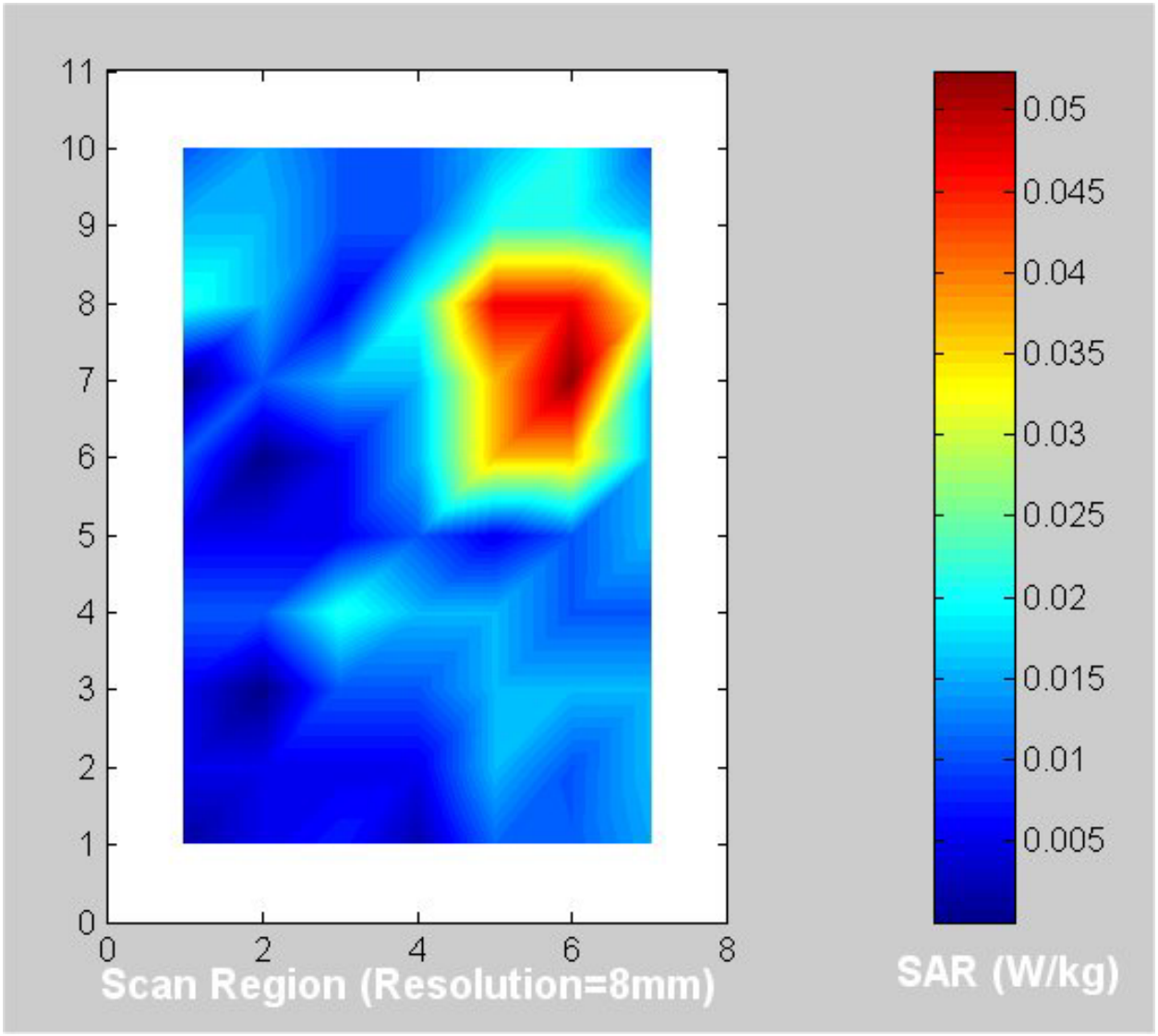

c. 5.745 GHz normal mode (see Table 7 for the peak 1-g SAR).

Fig. 18. Coarse scans for the SAR measurements for the **Above-lap** Configuration 1 of the Quantatw Model ZG1S PC with Ambit Model ZG1S 802.11a antenna. As shown in Fig. 4, the bottom of the Quantatw Model ZG1S PC is pressed against the base of the planar phantom for these measurements.

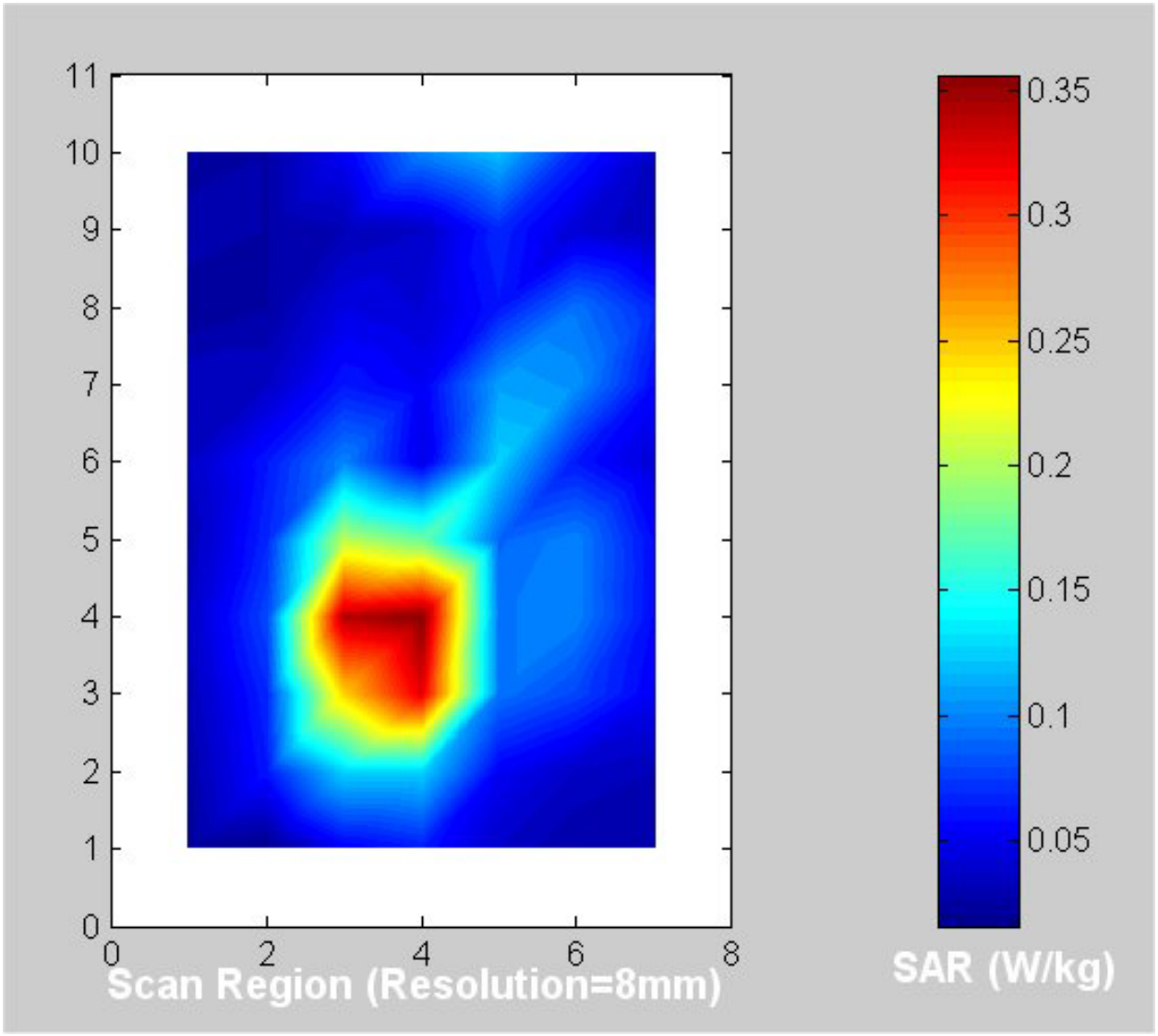

a. 5.20 GHz normal mode (see Table 8 for the peak 1-g SAR).

Fig. 19. Coarse scans for the SAR measurements for the **End-on** Configuration 3 of the Quantatw Model ZG1S PC with Ambit Model ZG1S 802.11a antenna. As shown in Fig. 10, the broader back edge of the PC at 90° is pressed against the bottom of the planar phantom with separation of 0 cm.

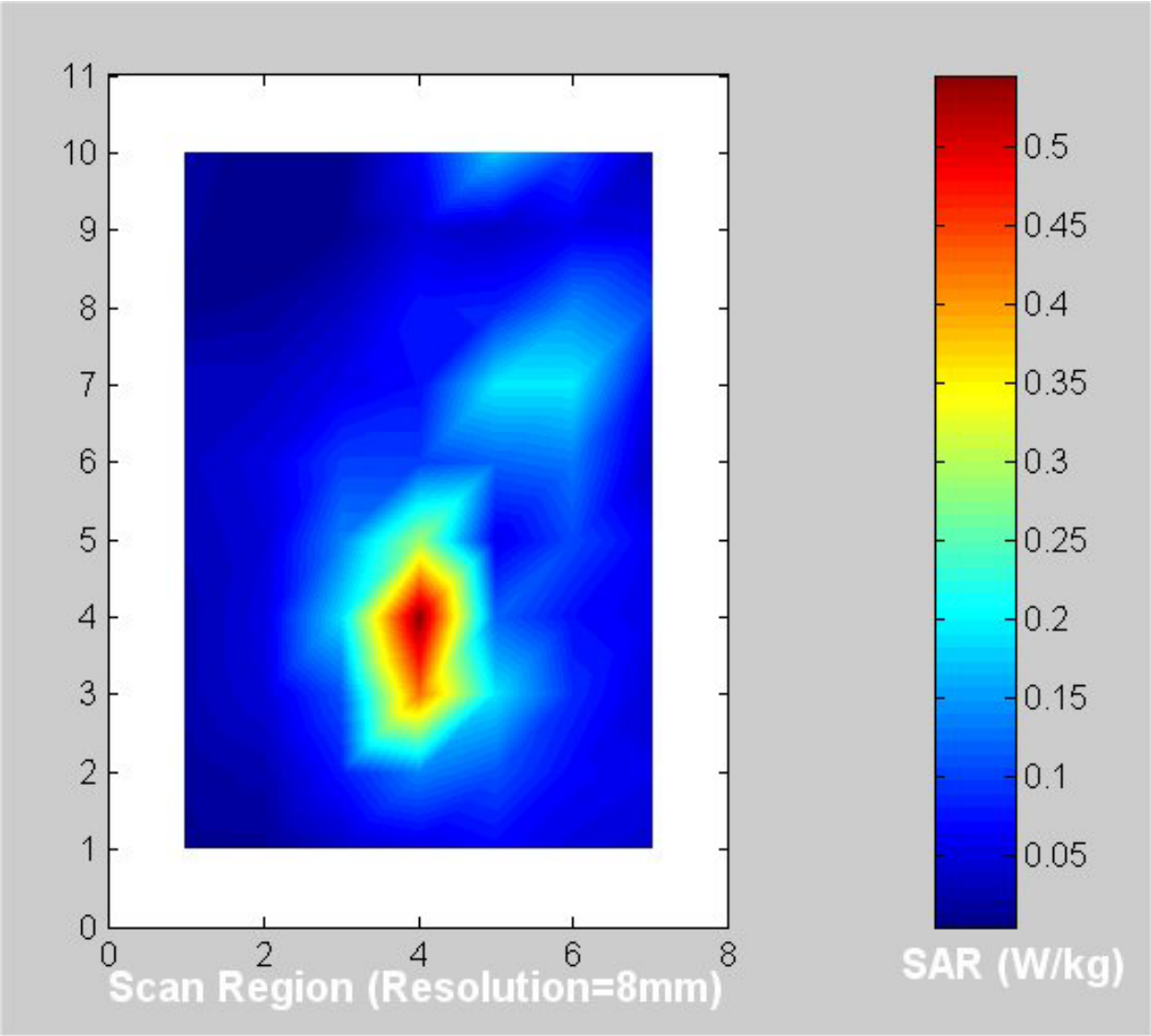

b. 5.30 GHz normal mode (see Table 9 for the peak 1-g SAR).

Fig. 19. Coarse scans for the SAR measurements for the **End-on** Configuration 3 of the Quantatw Model ZG1S PC with Ambit Model ZG1S 802.11a antenna. As shown in Fig. 10, the broader back edge of the PC at 90° is pressed against the bottom of the planar phantom with separation of 0 cm.

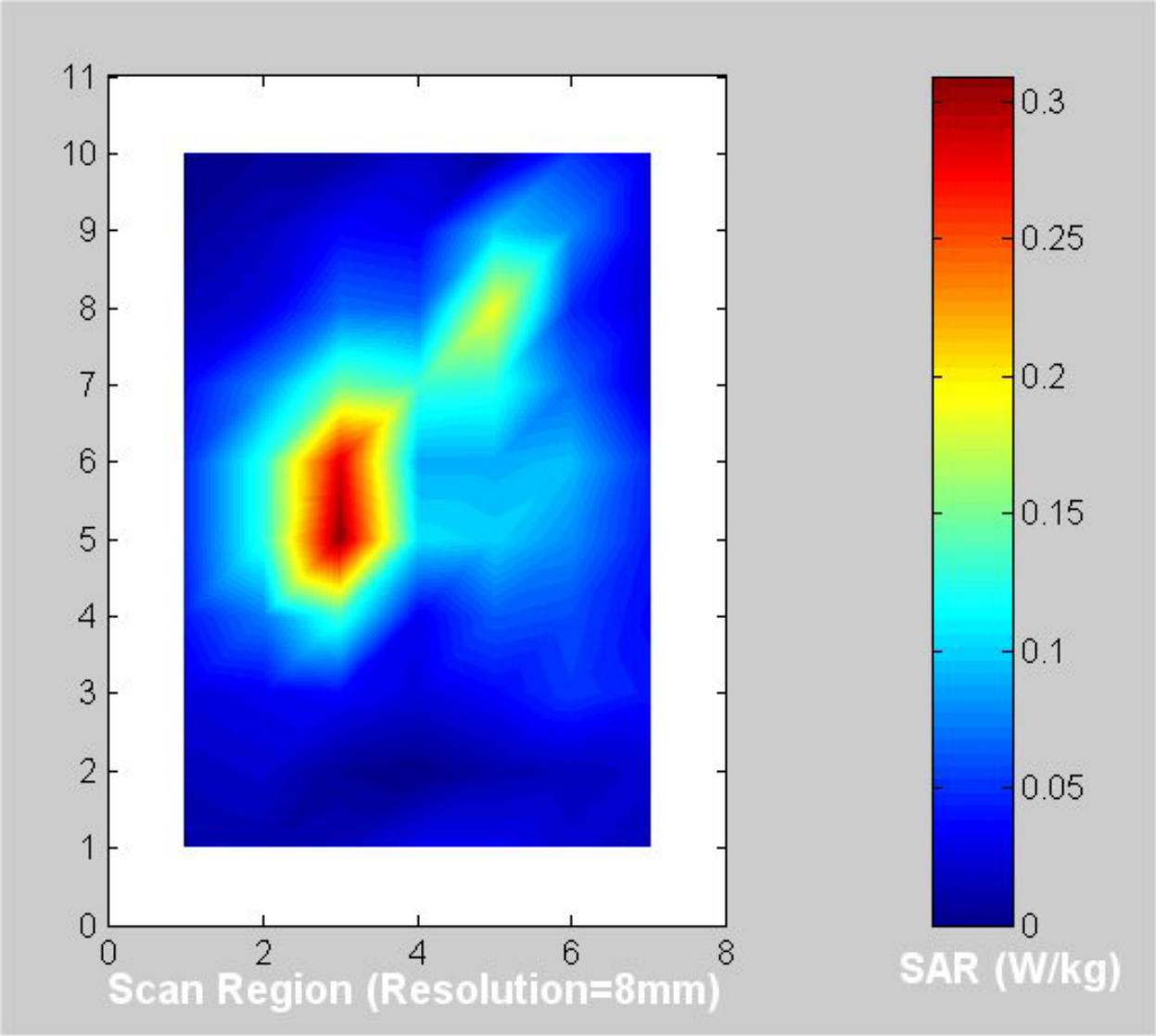

c. 5.745 GHz normal mode (see Table 10 for the peak 1-g SAR).

Fig. 19. Coarse scans for the SAR measurements for the **End-on** Configuration 3 of the Quantatw Model ZG1S PC with Ambit Model ZG1S 802.11a antenna. As shown in Fig. 10, the broader back edge of the PC at 90° is pressed against the bottom of the planar phantom with separation of 0 cm.

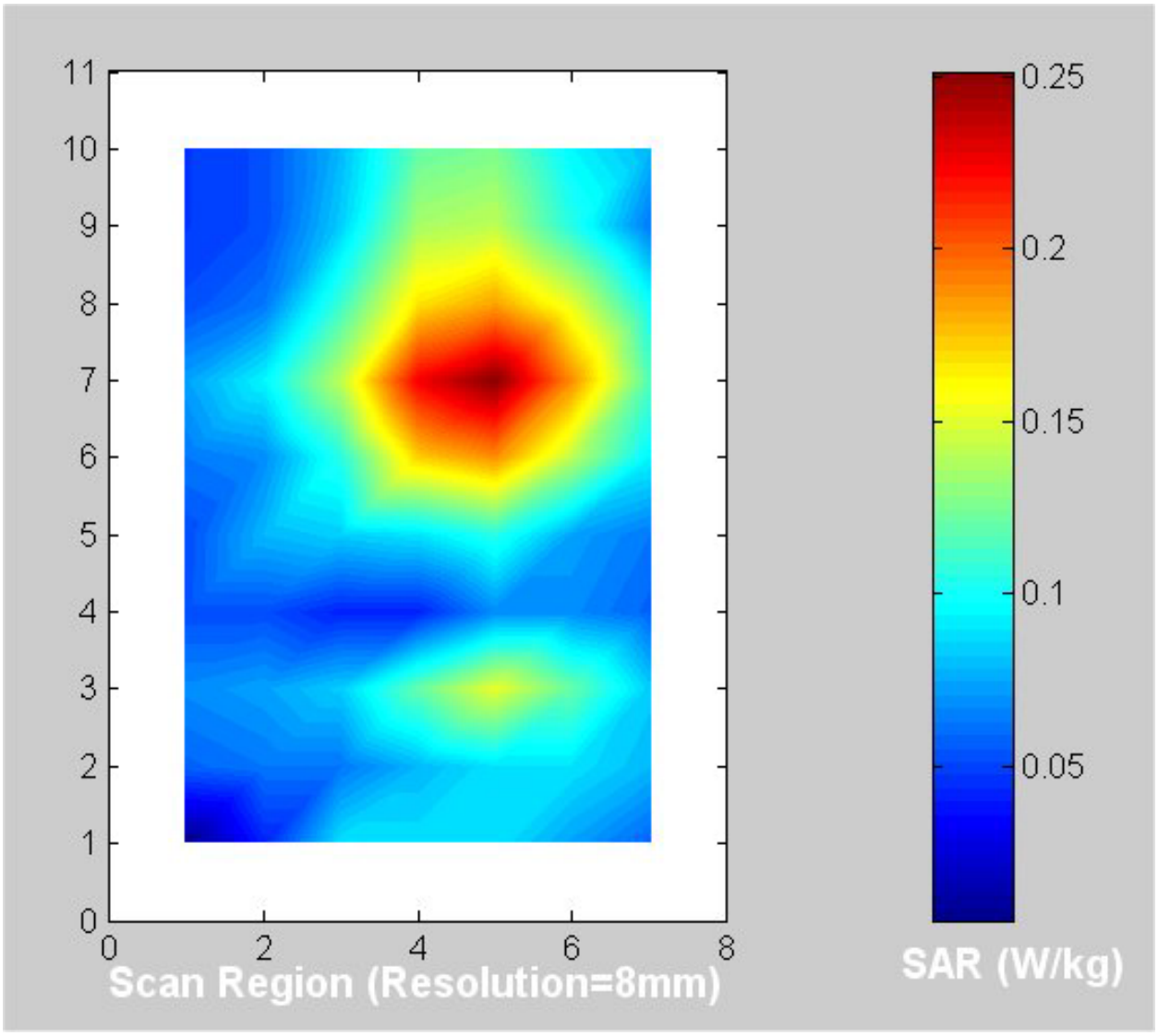

a. 5.20 GHz normal mode (see Table 11 for the peak 1-g SAR).

Fig. 20. Coarse scans for the SAR measurements for the **Edge-on** Configuration 2 of the Compal Model L1S PC with Ambit Model BY27 802.11a antenna. As shown in Fig. 9, the right antenna edge of the PC is parallel to the base of the planar phantom with a separation of 1.5 cm for these measurements.

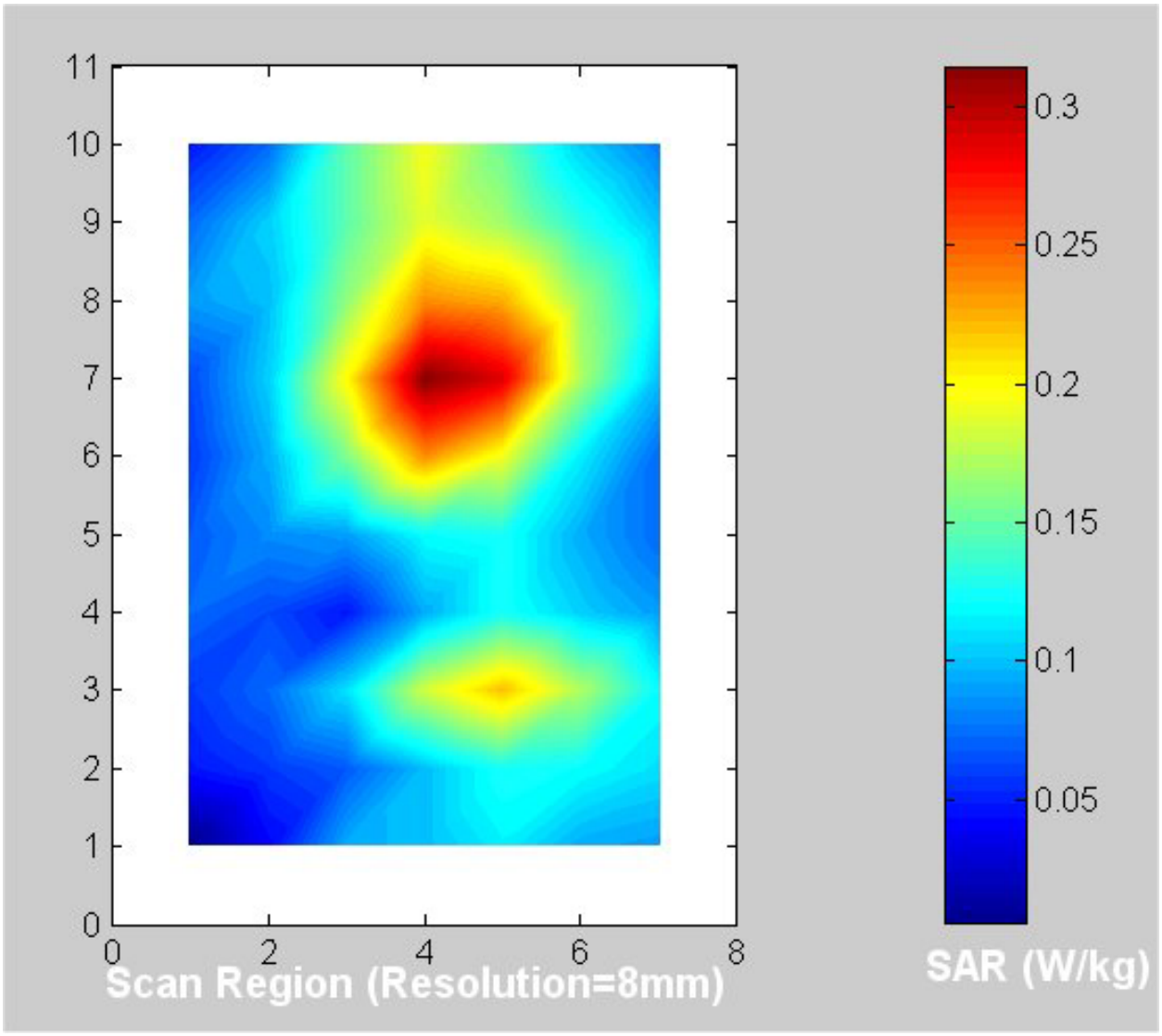

b. 5.30 GHz normal mode (see Table 12 for the peak 1-g SAR).

Fig. 20. Coarse scans for the SAR measurements for the **Edge-on** Configuration 2 of the Compal Model L1S PC with Ambit Model BY27 802.11a antenna. As shown in Fig. 9, the right antenna edge of the PC is parallel to the base of the planar phantom with a separation of 1.5 cm for these measurements.

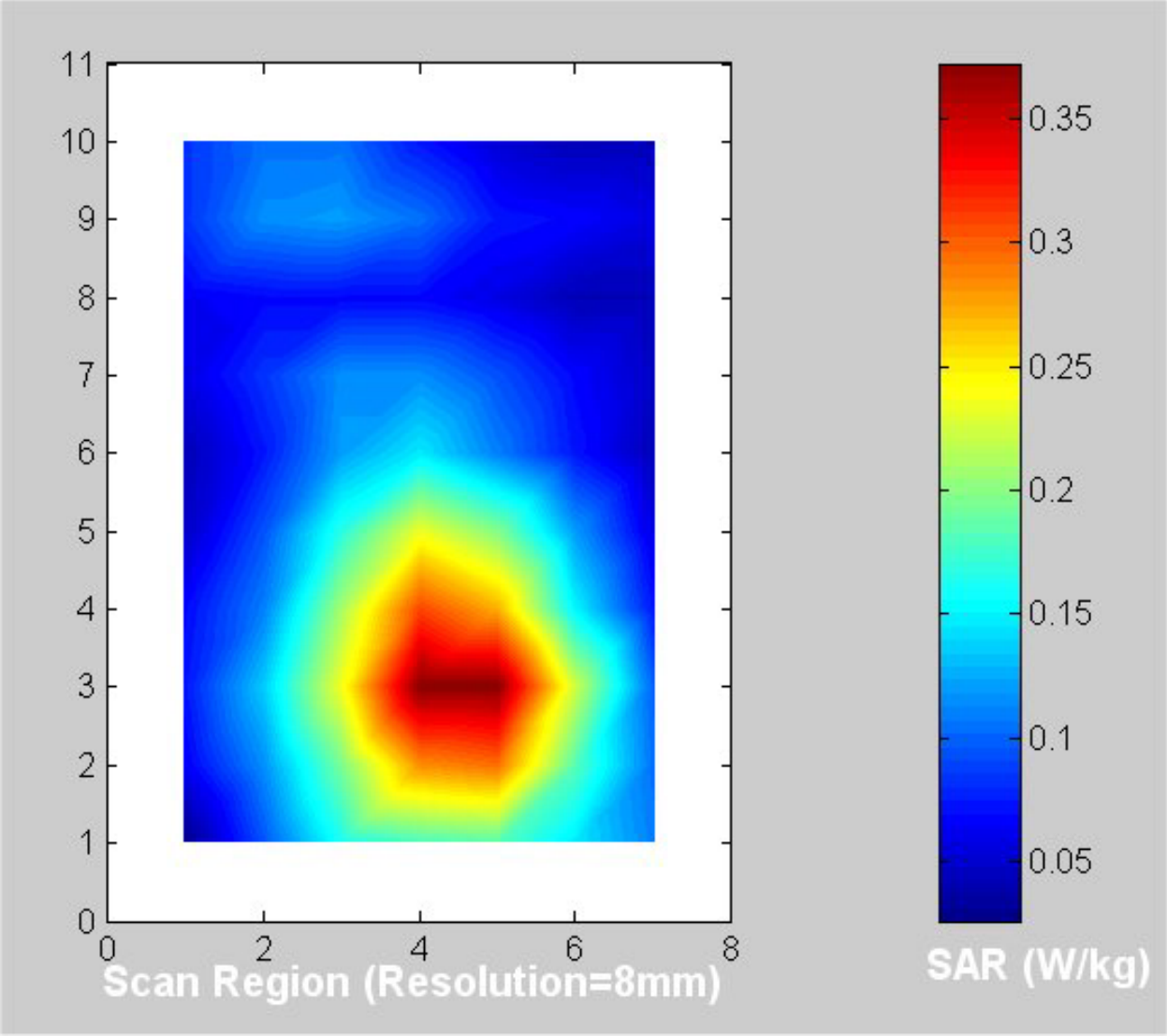

c. 5.745 GHz normal mode (see Table 13 for the peak 1-g SAR).

Fig. 20. Coarse scans for the SAR measurements for the **Edge-on** Configuration 2 of the Compal Model L1S PC with Ambit Model BY27 802.11a antenna. As shown in Fig. 9, the right antenna edge of the PC is parallel to the base of the planar phantom with a separation of 1.5 cm for these measurements.

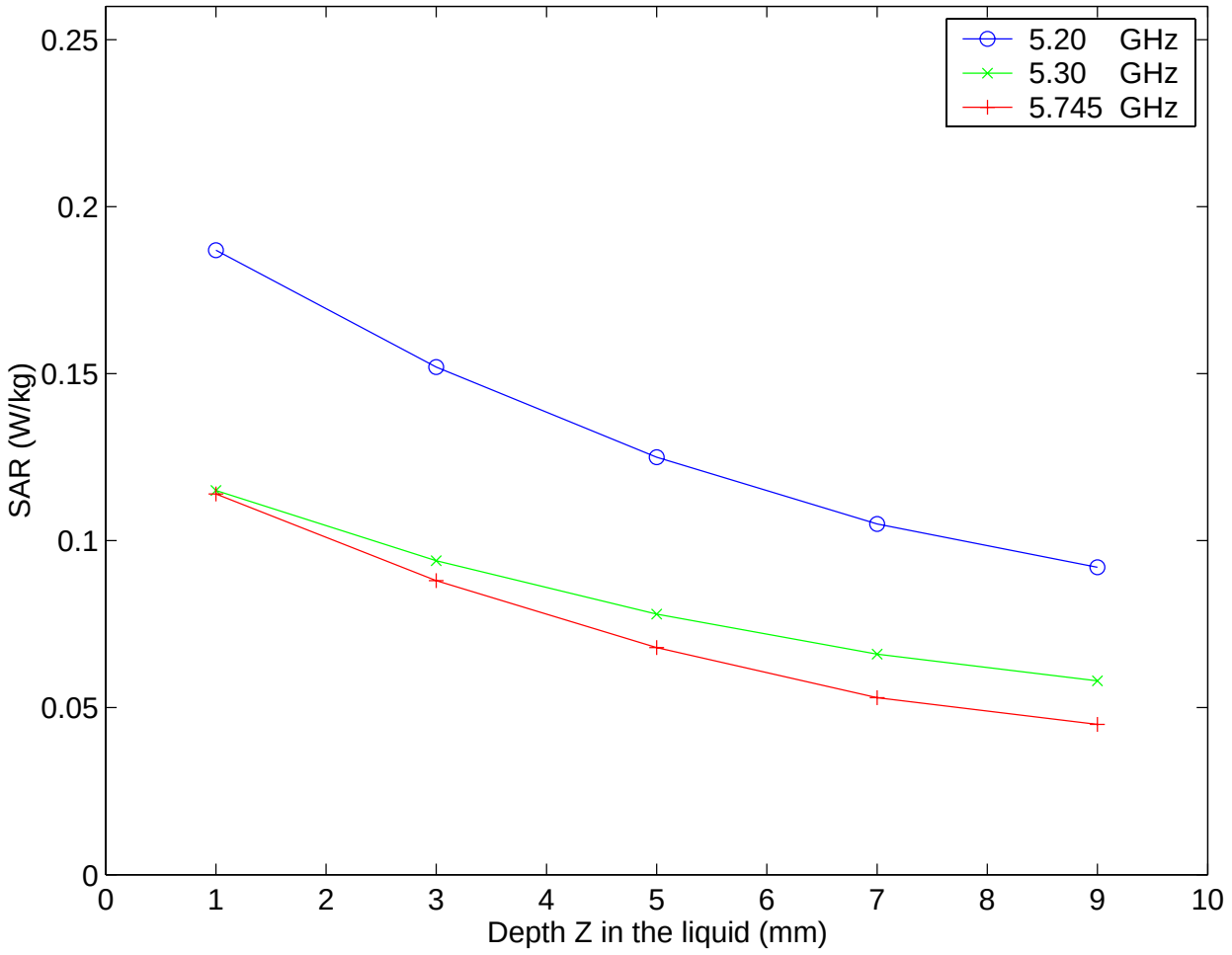

Fig. 21. Plot of the SAR variations as a function of depth Z in the liquid for locations of the highest SAR (from Tables 5-7) for Configuration 1 (Above-lap position – see Fig. 4) for Quantatw Model ZG1S PC with Ambit Model ZG1S 802.11a Antenna.

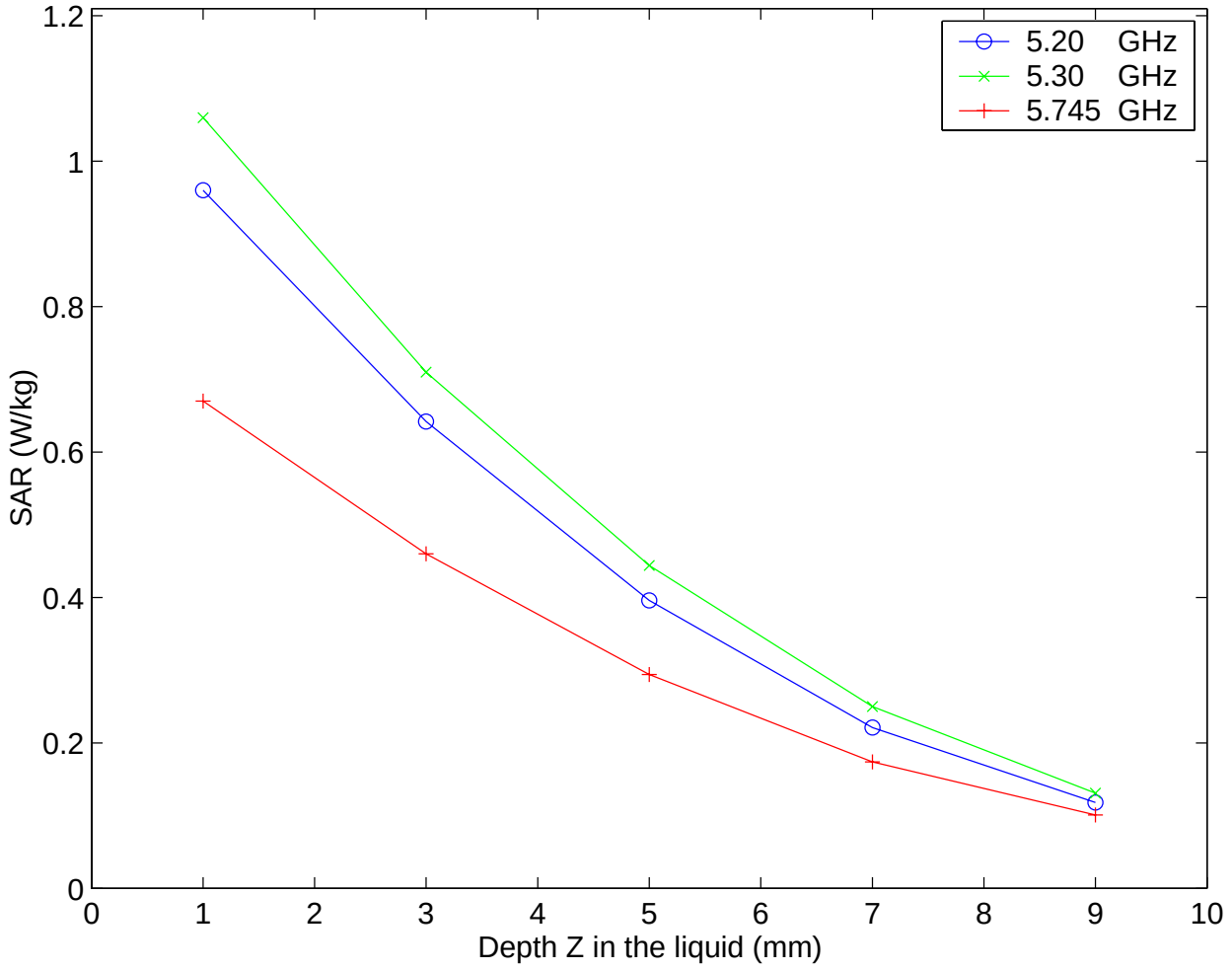

Fig. 22. Plot of the SAR variations as a function of depth Z in the liquid for locations of the highest SAR (from Tables 8-10) for Configuration 3 (End-on position – see Fig. 10) of Quantatw Model ZG1S PC with Ambit Model ZG1S 802.11a Antenna.

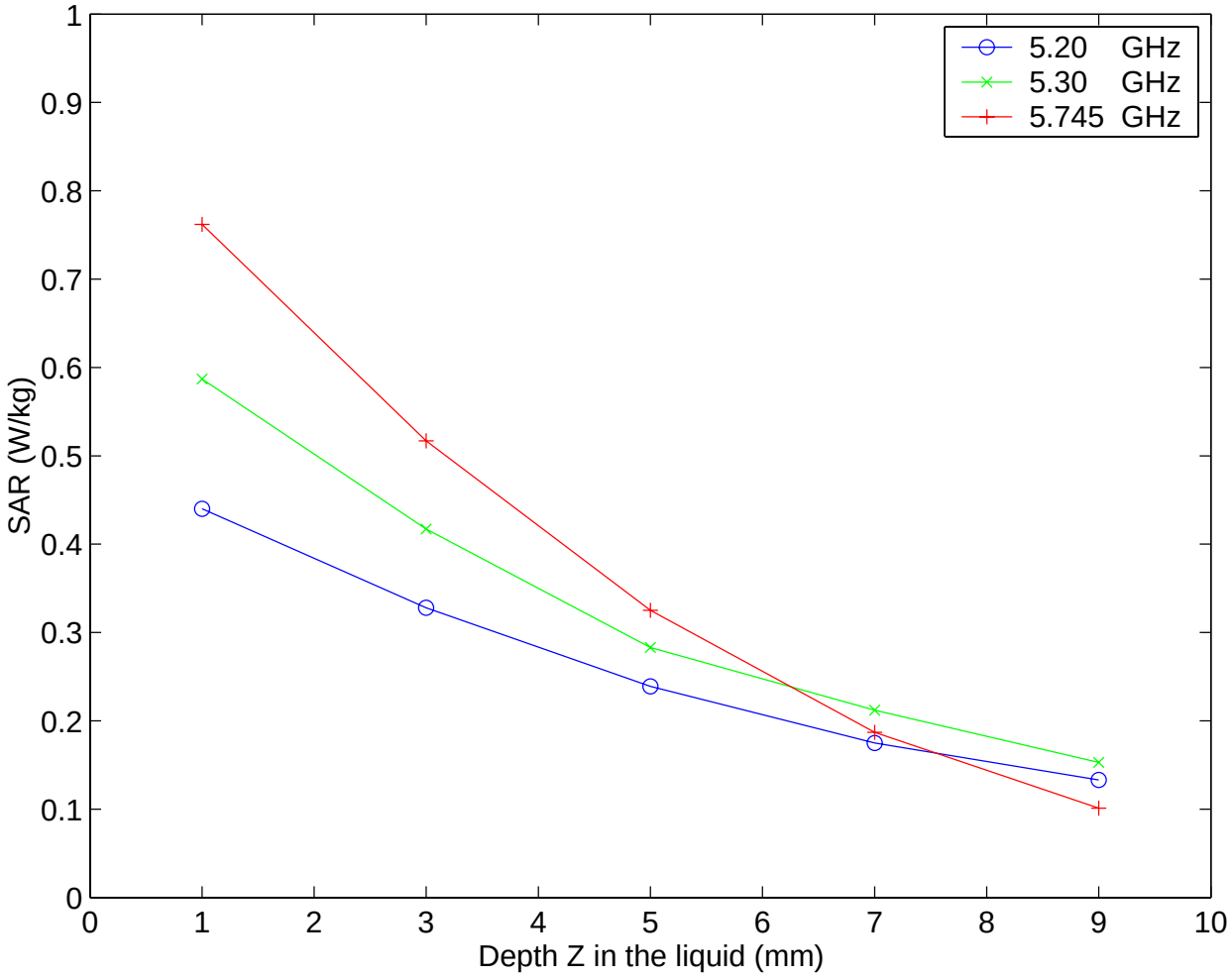

Fig. 23. Plot of the SAR variations as a function of depth Z in the liquid for locations of the highest SAR (from Tables 11-13) for Configuration 2 (Edge-on position – see Fig. 9) of Compal Model L1S PC with Ambit Model BY27 802.11a Antenna.

SAR System Verification for February 21, 2003

The measured SAR distribution for the peak 1-g SAR region using a dipole at 1900 MHz

For February 21, 2003 – The dipole SAR Plot

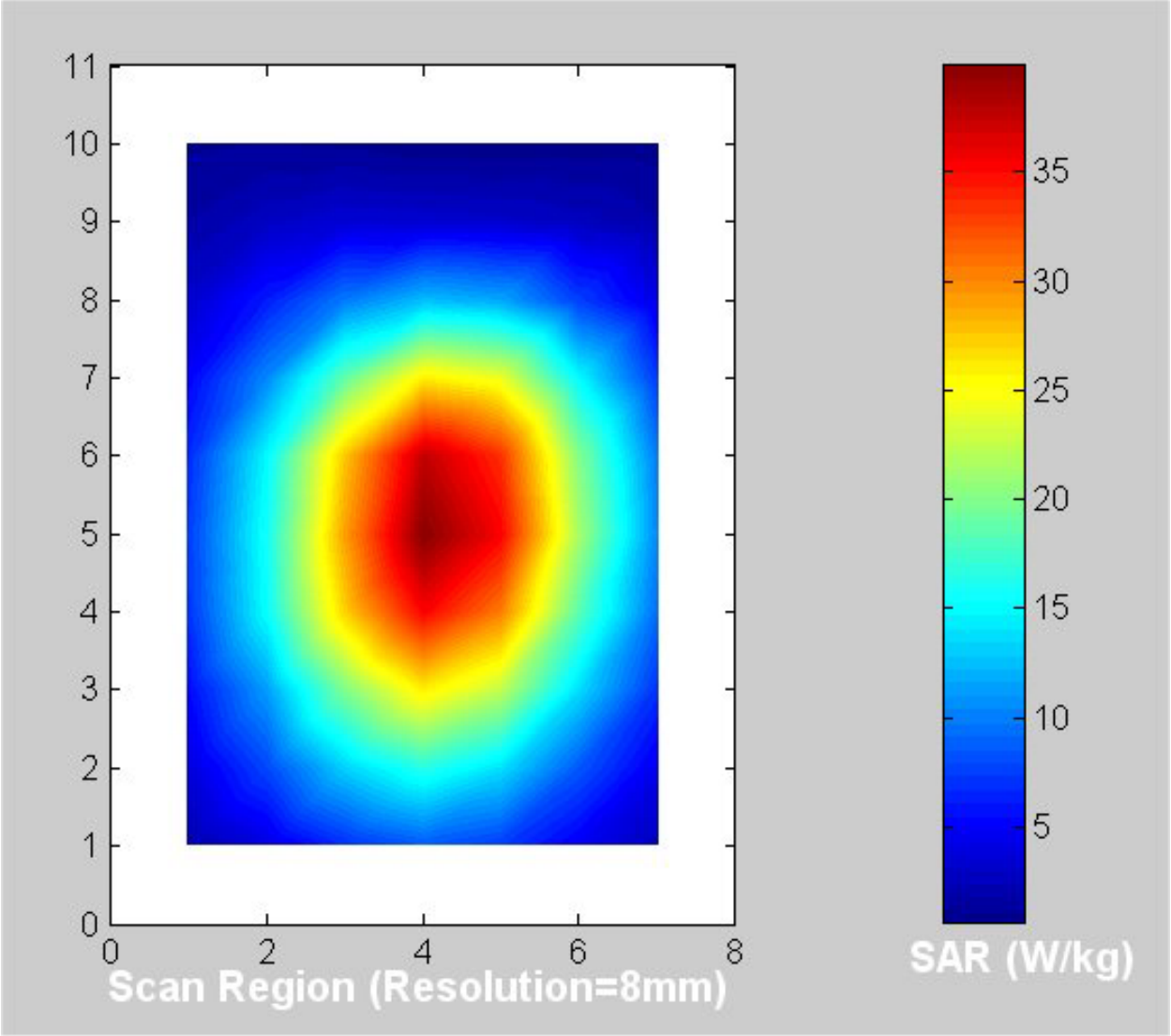

1-g SAR = 35.979 W/kg

a. At depth of 1 mm

54.143	56.392	57.404	56.574	54.080
55.086	57.536	58.513	57.844	55.318
55.196	57.780	58.817	58.201	55.667
54.754	57.145	58.314	57.694	55.286
53.621	56.172	57.331	56.996	54.539

b. At depth of 3 mm

42.511	44.157	44.889	44.270	42.444
43.358	45.125	45.840	45.322	43.488
43.543	45.411	46.138	45.685	43.830
43.217	44.982	45.816	45.375	43.590
42.410	44.255	45.111	44.822	43.036

c. At depth of 5 mm

32.666	33.819	34.319	33.876	32.596
33.422	34.633	35.131	34.741	33.466
33.657	34.937	35.422	35.098	33.797
33.434	34.682	35.244	34.942	33.671
32.891	34.158	34.765	34.520	33.280

d. At depth of 7 mm

24.607	25.377	25.693	25.391	24.537
25.279	26.059	26.387	26.101	25.250
25.537	26.358	26.666	26.438	25.567
25.404	26.244	26.597	26.394	25.530
25.064	25.882	26.293	26.090	25.273

e. At depth of 9 mm

18.336	18.831	19.012	18.815	18.267
18.928	19.404	19.608	19.401	18.842
19.184	19.673	19.872	19.706	19.141
19.127	19.670	19.877	19.731	19.166
18.929	19.426	19.695	19.532	19.013

APPENDIX C

Uncertainty Analysis

The uncertainty analysis of the University of Utah SAR Measurement System is given in Table A.1. Several of the numbers on tolerances are obtained by following procedures similar to those detailed in [8], while others have been obtained using methods suggested in [4].

Table B.1. Uncertainty analysis of the University of Utah SAR Measurement System.

Uncertainty Component	Tolerance ± %	Prob. Dist.	Div.	C_i 1-g	1-g u_i ± %
Measurement System					
Probe calibration	2.0	N	1	1	2.0
Axial istropy	4.0	R	$\sqrt{3}$	$(1\text{-}cp)^{1/2}$	1.6
Hemispherical isotropy	5.5	R	$\sqrt{3}$	$\sqrt{c_p}$	0.0
Boundary effect	0.8	R	$\sqrt{3}$	1	0.5
Linearity	3.0	R	$\sqrt{3}$	1	1.7
System detection limits	1.0	R	$\sqrt{3}$	1	0.6
Readout electronics	1.0	N	1	1	1.0
Response time	0.0	R	$\sqrt{3}$	1	0.0
Integration time	0.5	R	$\sqrt{3}$	1	0.3
RF ambient conditions	0	R	$\sqrt{3}$	1	0
Probe positioner mechanical tolerance	0.5	R	$\sqrt{3}$	1	0.3
Probe positioning with respect to phantom shell	2.0	R	$\sqrt{3}$	1	1.2
Extrapolation, interpolation, and integration algorithms for max. SAR evaluation	5.0	R	$\sqrt{3}$	1	2.9
Test Sample Related					
Test sample positioning	3	R	$\sqrt{3}$	1	1.7
Device holder uncertainty	3	R	$\sqrt{3}$	1	1.7
Output power variation - SAR drift measurement	5	R	$\sqrt{3}$	1	2.9
Phantom and Tissue Parameters					
Phantom uncertainty - shell thickness tolerance	10.0	R	$\sqrt{3}$	1	5.8
Liquid conductivity - deviation from target values	0.4	R	$\sqrt{3}$	0.7	0.2
Liquid conductivity - measurement uncertainty	1.5	R	$\sqrt{3}$	0.7	0.6
Liquid permitivity - deviation from target values	0.8	R	$\sqrt{3}$	0.6	0.3
Liquid permittivity - measurement uncertainty	3.5	R	$\sqrt{3}$	0.6	1.2
Combined Standard Uncertainty		RSS			8.3
Expanded Uncertainty (95% Confidence Level)					16.6